Recent Subsidence and Erosion at Diverse Wetland Sites in the Southeastern Mississippi Delta Plain

By Robert A. Morton, Julie C. Bernier, and Kyle W. Kelso

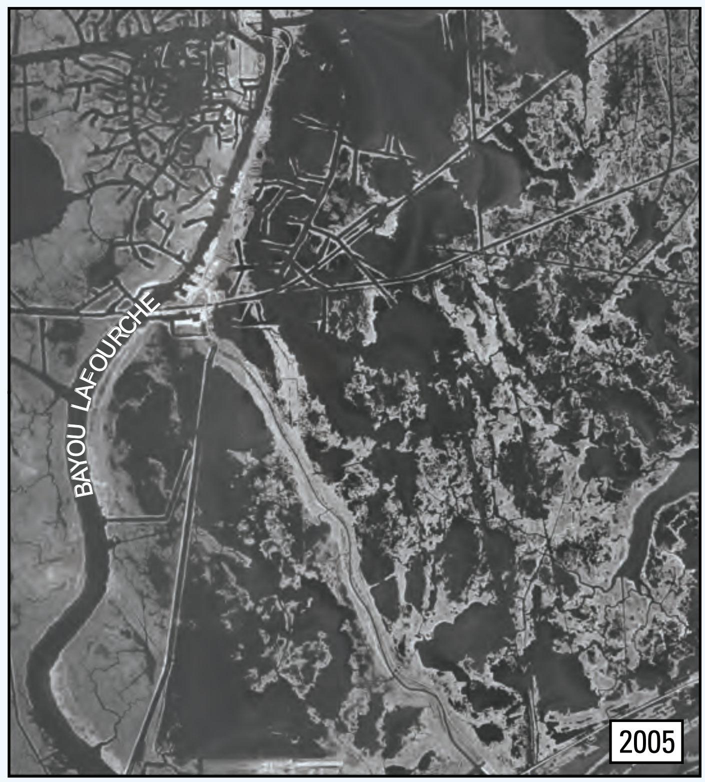

Open-File Report 2009-1158

U.S. Department of the Interior
U.S. Geological Survey

Cover. Aerial photographs from 1958 and 2005 illustrate the extent of wetland loss in the lower Mississippi delta plain east of Bayou Lafourche, Lafourche Parish, Louisiana. Scale 1:100,000

Recent Subsidence and Erosion at Diverse Wetland Sites in the Southeastern Mississippi Delta Plain

By Robert A. Morton, Julie C. Bernier, and Kyle W. Kelso

Open-File Report 2009-1158

U.S. Department of the Interior
U.S. Geological Survey

U.S. Department of the Interior
KEN SALAZAR, Secretary

U.S. Geological Survey
Suzette M. Kimball, Acting Director

U.S. Geological Survey, Reston, Virginia: 2009

For more information on the USGS—the Federal source for science about the Earth, its natural and living resources, natural hazards, and the environment, visit *http://www.usgs.gov* or call 1-888-ASK-USGS

For an overview of USGS information products, including maps, imagery, and publications, visit *http://www.usgs.gov/pubprod*

To order this and other USGS information products, visit *http://store.usgs.gov*

Suggested citation:
Morton, R.A., Bernier, J.C., and Kelso, K.W., 2009, Recent subsidence and erosion at diverse wetland sites in the southeastern Mississippi delta plain: U.S. Geological Survey Open-File Report, 2009–1158, 39 p., plus app. (p. 41-221).

ISBN 978-1-4113-2529-6

Contents

Figures

Tables

Conversion Factors

Multiply	By	To obtain
	Length	
centimeter (cm)	0.3937	inch (in.)
meter (m)	3.281	foot (ft)
kilometer (km)	0.6214	mile (mi)

Vertical coordinate information is referenced to the North American Vertical Datum of 1988 (NAVD88).

Horizontal coordinate information is referenced to the North American Datum of 1983 (NAD83).

Recent Subsidence and Erosion at Diverse Wetland Sites in the Southeastern Mississippi Delta Plain

By Robert A. Morton[1], Julie C. Bernier[2], and Kyle W. Kelso[3]

Abstract

A prior study (U.S. Geological Survey Open-File Report 2005-1216) examined historical land- and water-area changes and estimated magnitudes of land subsidence and erosion at five wetland sites in the Terrebonne hydrologic basin of the Mississippi delta plain. The present study extends that work by analyzing interior wetland loss and relative magnitudes of subsidence and erosion at five additional wetland sites in the adjacent Barataria hydrologic basin. The Barataria basin sites were selected for their diverse physical settings and their recent (post-1978) conversion from marsh to open water. Historical aerial photography, datum-corrected marsh elevations and water depths, sediment cores, and radiocarbon dates were integrated to evaluate land-water changes in the Mississippi delta plain on both historical and geological time scales.

The thickness of the organic-rich sediments (peat) and the elevation of the stratigraphic contact between peat and underlying mud were compared at marsh and open-water sites across areas of formerly continuous marsh to estimate magnitudes of recent delta-plain elevation loss caused by vertical erosion and subsidence of the wetlands. Results of these analyses indicate that erosion exceeded subsidence at most of the study areas, although both processes have contributed to historical wetland loss. Comparison of these results with prior studies indicates that subsidence largely caused rapid interior wetland loss in the Terrebonne basin before 1978, whereas erosional processes primarily caused more gradual interior wetland loss in the Barataria basin after 1978.

Decadal variations in rates of relative sea-level rise at a National Ocean Service tide gage, elevation changes between repeat benchmark-leveling surveys, and GPS height monitoring at three National Geodetic Survey Continuously Operating Reference Stations indicate that subsidence rates since the early 1990s are substantially lower than those previously reported and are similar in magnitude to time-averaged subsidence rates at geological time scales. The historical decrease in land-loss rates across the Mississippi delta plain generally is consistent with the recent decrease in subsidence rates within the same region.

Introduction

Wetland loss in coastal Louisiana continues to be an ecological and economic concern for officials at all levels of government. The conversion of land to open water is so extensive and the causes are so diverse that coastal-restoration efforts require many different projects and multiple approaches (National Research Council, 2006). Despite recent findings that indicate significant decline in the rate of wetland loss (Morton and others, 2005; Barras and others, 2008), average annual losses and short-term losses associated with extreme events, such as Hurricanes Katrina and Rita in 2005, are still substantial (Barras and others, 2008).

Since 1999, the U.S. Geological Survey (USGS) has been conducting research directed toward a better understanding of the physical processes that contribute to wetland loss in the Gulf Coast region. Recent USGS efforts have focused on hotspot areas of the Mississippi delta plain, where high rates of interior wetland loss are difficult to explain when only surficial processes and wetland ecology are considered. Prior USGS studies that examined the temporal and spatial distribution of interior wetland loss in Lafourche and Terrebonne Parishes in Terrebonne basin demonstrated close temporal and spatial correlations between wetland loss, delta-plain subsidence, and deep-subsurface hydrocarbon production (Morton and others, 2003; 2005; 2006). Those prior studies investigated areas where rapid delta-plain wetland loss occurred primarily between the mid-1960s and 1978 – a period when oil and gas production in the same areas rapidly accelerated and peaked (Morton and others, 2005; 2006).

During 2006 and 2007, USGS field investigations of subsidence within the Barataria basin of the southeastern Mississippi delta plain focused on five areas (figs. 1 and 2) where significant wetland loss occurred after 1978 (figs. 3 and 4). The five study areas encompassed a spectrum of geological settings including: (1) an interior open-water body (Bayou Perot, Lafourche and Jefferson Parishes), (2) a site adjacent to the modern levee of the Mississippi River (Ironton, Jefferson Parish), (3) two lower delta-plain sites (Leeville and Fourchon, Lafourche Parish), and (4) a beach-ridge margin site (Caminada, Lafourche Parish).

[1]U.S. Geological Survey, 10100 Burnet Rd., Bldg. 130, Austin, Texas 78758

[2]U.S. Geological Survey, Florida Integrated Science Center, 600 4th St. South, St. Petersburg, FL 33701

[3]Jacobs Technology Inc., 600 4th St. South, St. Petersburg, Florida 33701

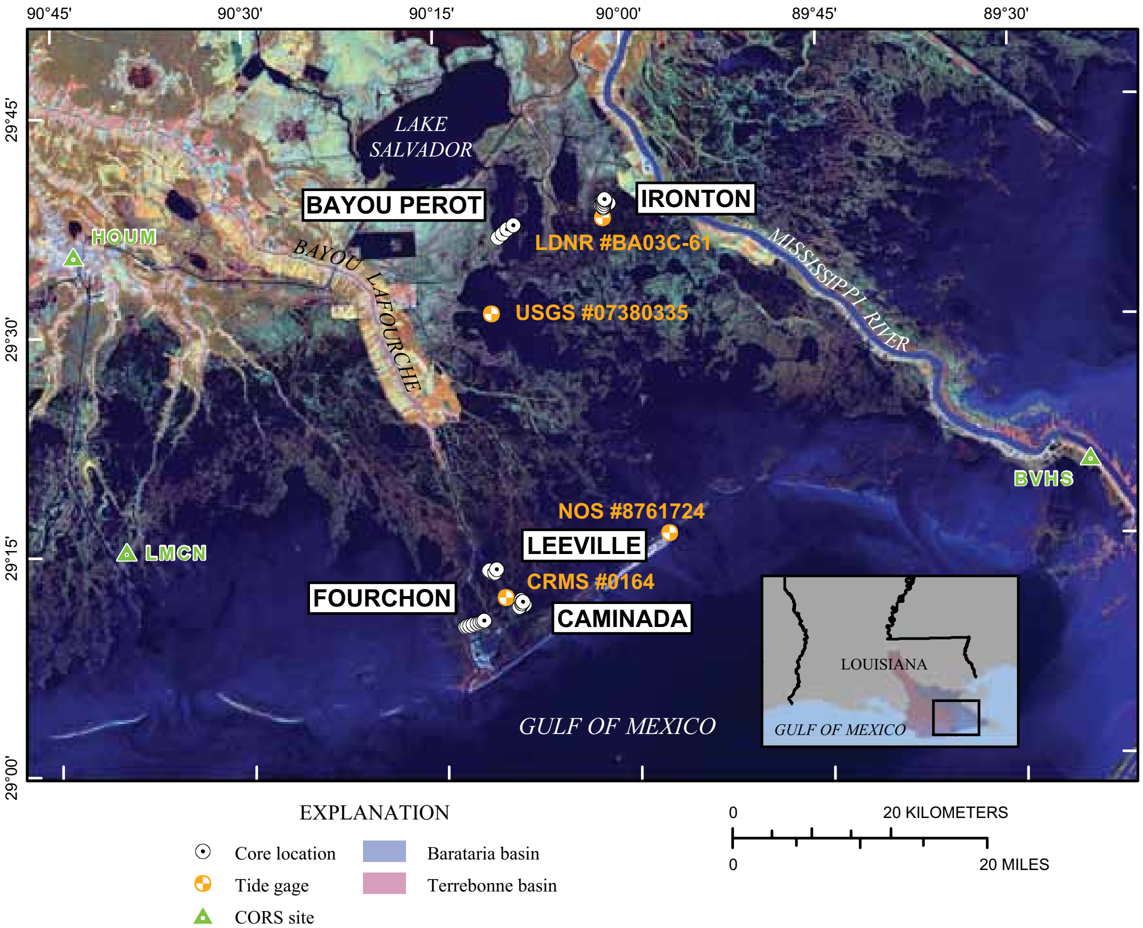

Figure 1. Regional map of the Barataria and Terrebonne hydrologic basins in southeastern Louisiana showing locations of coring sites relative to nearby tide gages and Continuously Operating Reference Stations (CORS). Landsat 5 Thematic Mapper (TM) image acquired October 28, 2006; RGB visual display uses bands 4 (near-infrared), 5 (mid-infrared), and 3 (visible red). CORS sites: BVHS, Boothville; HOUM, Houma; LMCN, Cocodrie.

The Bayou Perot and Ironton sites are middle-to-upper delta-plain interdistributary sites where marshes generally have persisted for thousands of years. The Leeville, Fourchon, and Caminada sites are on a lower delta-plain headland that is maintained by the natural levees and adjacent marshes of Bayou Lafourche, which lie between Barataria Bay to the east and Timbalier Bay to the west. Marshes of the lower delta plain are only a few hundred years old. As a result of these contrasting settings, the oldest marshes at Bayou Perot and Ironton are substantially older than the oldest marshes at Leeville, Fourchon, and Caminada.

Field and Laboratory Analyses

Fieldwork was conducted September 5-8, 2006, September 6-8, 2007, and October 8-10, 2007. The fieldwork involved collecting vibracores and push cores and measuring water depths at the Bayou Perot, Ironton, Leeville, Fourchon, and Caminada study areas (figs. 1 and 2).

Coring Operations

Both vibracores and push cores were used to determine the thickness and characteristics of shallow sediments beneath the delta plain. Vibracores are designated ‘v’ and push cores are designated ‘p’, respectively, after the core identification code (tables 1 and 2; appendix). More than one core was collected at some coring sites, so the ‘p’ and ‘v’ designations are not used when referring to a site rather than to individual cores. The vibracoring technique was illustrated and described by Lanesky and others (1979). Vibracores were taken at both the emergent-marsh sites and also from a coring barge at the open-water sites where water depths prevented the collection of push cores. Compared to push cores, vibracores provide deeper, continuous penetration, which can reveal stratigraphy below the thick, organic-rich sediments that occur near the surface.

A Russian peat corer (Jowsey, 1966) was used to collect sediment cores at each of the emergent-marsh coring sites. The peat corer is a manually operated, side-filling sampler that is designed to minimize compaction and core shortening because

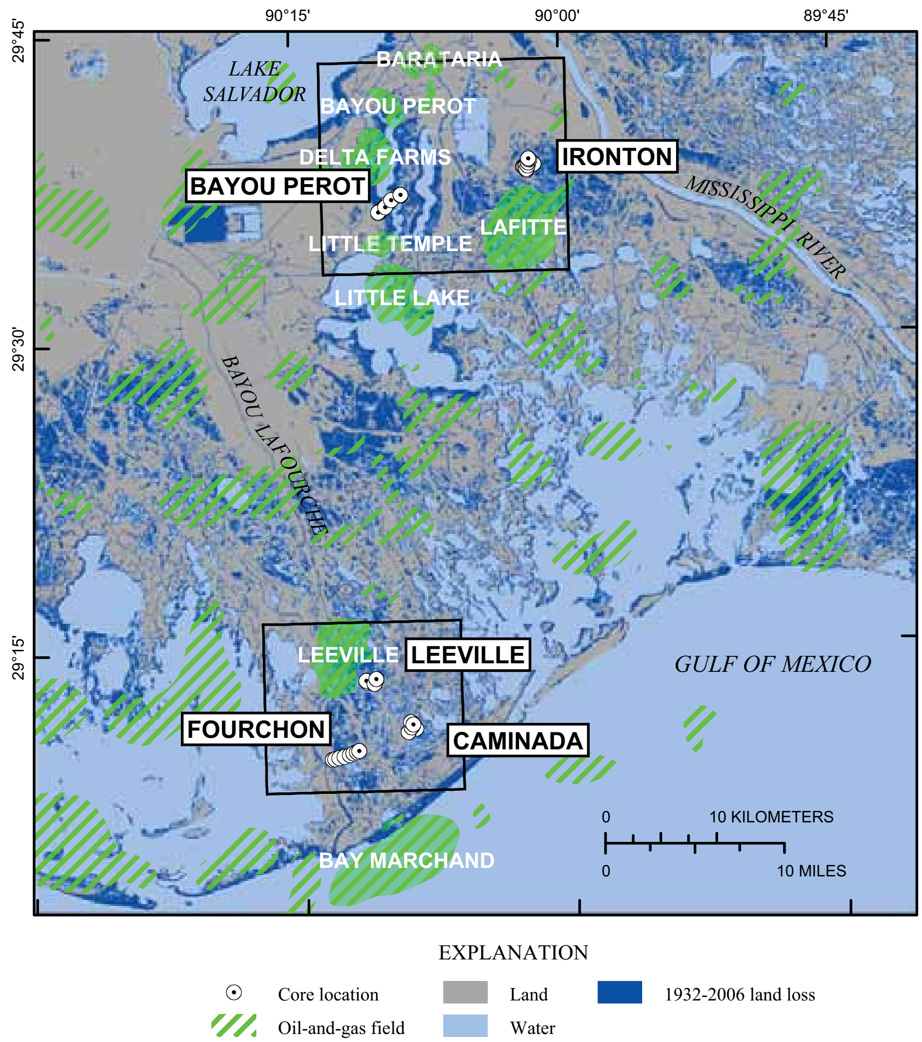

Figure 2. Regional map of the Barataria and Terrebonne hydrologic basins in southeastern Louisiana showing locations of coring sites, oil-and-gas fields, and historical wetland loss from 1932 to 2006. Boxed areas show the locations of figures 3 and 4.

the collection tube is inserted adjacent to the sediment interval being extracted. To avoid sediment contamination, the collection tube remains closed until the desired sampling depth is reached. As the handle is rotated 180° clockwise, a leading blade cuts through the sediment until it reaches the cover plate, which encloses the sediment within the collection tube.

When possible, the push corer was inserted into the same hole left by extraction of the previous core in order to limit resistance against the coring device and to ensure recovery of the correct depth interval. However, at some locations, marsh sediments and water backfilled the hole, making it necessary to offset the corer approximately 15 centimeters (cm) and push the collection tube to the depth of the preceding sample to continue the coring operation. Each 1-meter (m) core section was transferred into pre-cut, semi-cylindrical PVC pipe. The cores were then encased in plastic wrap, sealed to retain moisture, and labeled according to study site, depth, and orientation.

Seventy-four vibracores and 16 push cores were located with a portable Global Positioning System (GPS) receiver within the study areas where historical wetland loss has been rapid and widespread. Cores taken across the perimeter of the hotspots provided close stratigraphic correlation between the present emergent marsh and adjacent open water where emergent marsh formerly existed.

The cores were transported to the USGS Florida Integrated Science Center in St. Petersburg, FL. Each vibracore was cut into 1-m sections and split lengthwise. One-half of each core was cleaned, photographed, and described in detail. The other half was immediately sealed for future sampling procedures such as isotopic analysis. All core sections were then placed in containers and stored. Core descriptions and photographs (appendix) were used to identify the predominant sedimentary facies and to select stratigraphic contacts that were correlated between cores and used to estimate magnitudes of wetland subsidence and erosion (table 1).

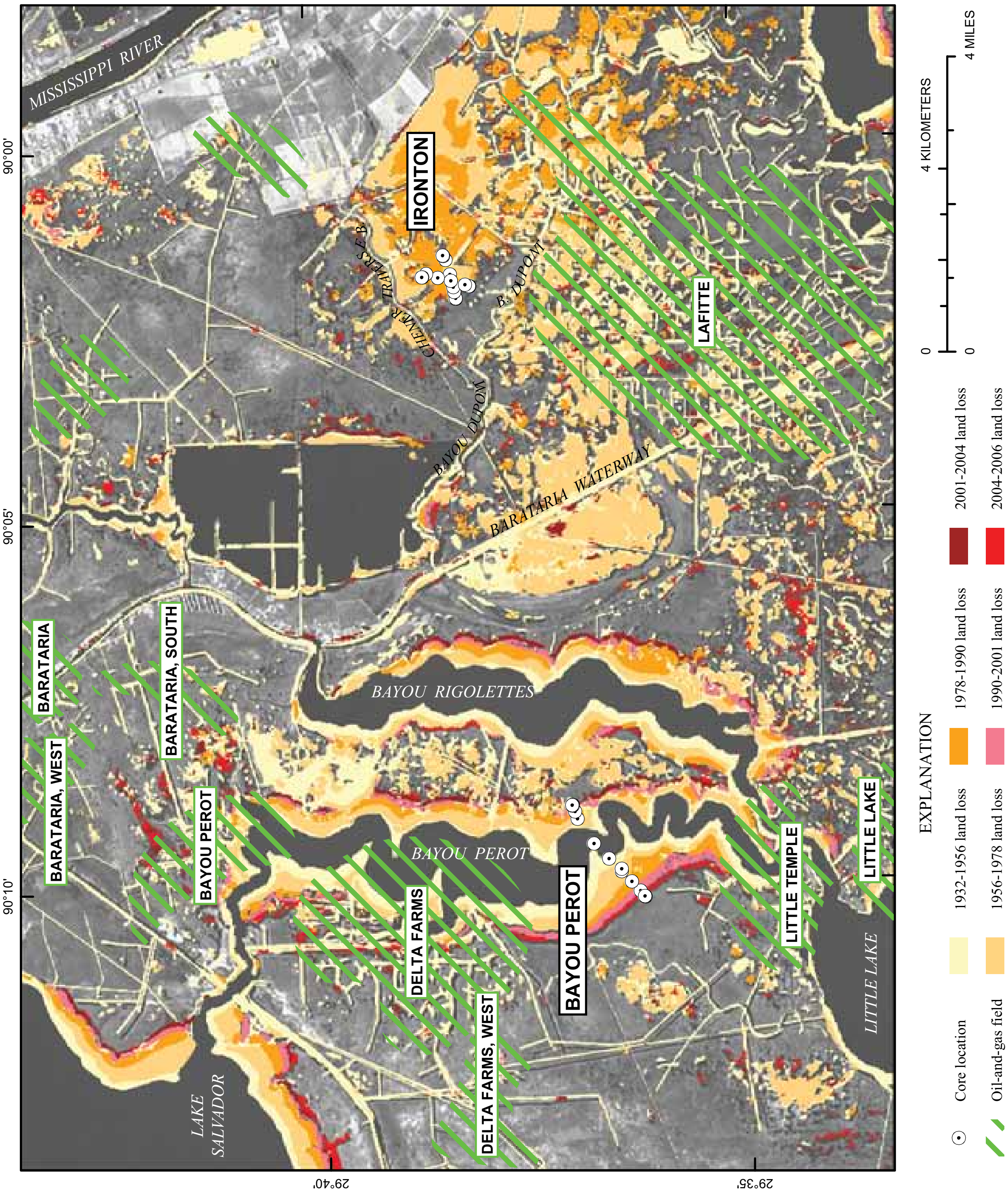

Figure 3. Map of central Barataria basin showing location of Bayou Perot and Ironton coring sites, oil-and-gas fields, and historical land-loss trends between 1932 and 2006. Wetland loss trends from Barras and others (2008) and John Barras (personal commun., 2008); Landsat 5 Thematic Mapper (TM) image acquired October 28, 2006; display uses band 5 (mid-infrared).

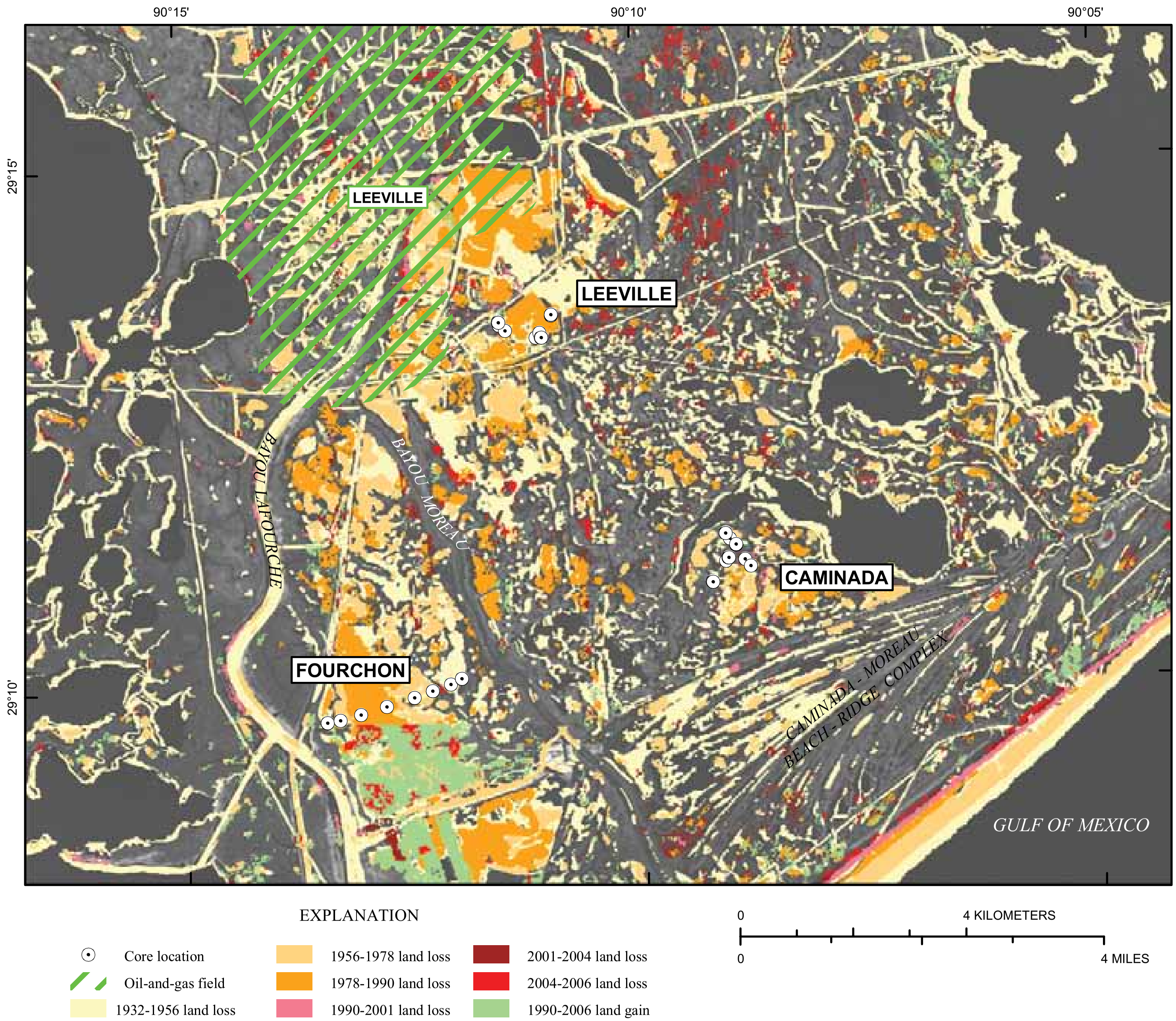

Figure 4. Map of southern Barataria basin showing location of Fourchon, Caminada, and Leeville coring sites, Leeville oil-and-gas field, and composite historical land-water changes between 1932 and 2006. Landsat 5 Thematic Mapper (TM) image acquired October 28, 2006; display uses band 5 (mid-infrared).

Table 1. Adjusted core depths (thickness) and NAVD88 elevations for the base of the first marsh correlated between cores at Bayou Perot, Ironton, Leeville, Fourchon, and Caminada study areas.

[The linear adjustment method was used to decompact the cores. Positive marsh-minus-water (m-w) adjusted depth-difference values indicate erosion, and negative m-w depth-difference values indicate sediment accumulation; m-w adjusted elevation-difference values represent estimated subsidence. Cores are arranged in the same order that they are shown on the stratigraphic cross sections (figs. 7, 9, 10, 12, 14, 16, and 17); cm, centimeters]

Core ID	Core Location	Core Elevation (cm NAVD88)	Adjusted Depth (cm)	Adjusted Elevation (cm NAVD88)
Bayou Perot study area: transect BP-13p to BP-09p (fig. 7)				
BP-13p	marsh	31	336	-305
BP-14v	marsh edge	-91	236	-327
difference (m-w)		122	100	22
BP-13p	marsh	31	336	-305
BP-06v	water	-114	262	-376
difference (m-w)		145	74	71
BP-13p	marsh	31	336	-305
BP-05v	water	-143	219	-362
difference (m-w)		174	117	57
BP-13p	marsh	31	336	-305
BP-04v	water	-163	302	-465
difference (m-w)		194	34	160
BP-13p	marsh	31	336	-305
BP-03v	water	-171	223	-394
difference (m-w)		202	113	89
BP-09p	marsh	51	318	-267
BP-02v	water	-143	137	-280
difference (m-w)		194	181	13
BP-09p	marsh	51	318	-267
BP-01v	water	-127	161	-288
difference (m-w)		178	157	21
BP-09p	marsh	51	318	-267
BP-10v	marsh edge	-11	324	-335
difference (m-w)		62	-6	68
Ironton study area: transect IRN-01v to IRN-08v (fig. 9)				
IRN-01v	marsh	25	96	-71
IRN-02v	marsh edge	-10	112	-122
difference (m-w)		35	-16	51
IRN-01v	marsh	25	96	-71
IRN-03v	water	-48	83	-131
difference (m-w)		73	13	60
IRN-01v	marsh	25	96	-71
IRN-13v	water	-47	122	-169
difference (m-w)		72	-26	98

Table 1. Adjusted core depths (thickness) and NAVD88 elevations for the base of the first marsh correlated between cores at Bayou Perot, Ironton, Leeville, Fourchon, and Caminada study areas. —Continued

Core ID	Core Location	Core Elevation (cm NAVD88)	Adjusted Depth (cm)	Adjusted Elevation (cm NAVD88)
IRN-08v [1]	marsh edge	23	96	-73
IRN-05Bv	water	-57	55	-112
difference (m-w)		80	41	39
IRN-08v [1]	marsh edge	23	96	-73
IRN-06v	water	-47	61	-108
difference (m-w)		70	35	35
Ironton study area: transect IRN-15v to IRN-09v (fig. 10)				
IRN-15v	marsh	28	155	-127
IRN-16v	marsh edge	-12	117	-129
difference (m-w)		40	38	2
IRN-15v	marsh	28	155	-127
IRN-14v	water	-56	85	-141
difference (m-w)		84	70	14
IRN-15v	marsh	28	155	-127
IRN-13v	water	-47	122	-169
difference (m-w)		75	33	42
IRN-15v	marsh	28	155	-127
IRN-04v	water	-61	78	-139
difference (m-w)		89	77	12
IRN-15v	marsh	28	155	-127
IRN-12v	water	-64	95	-159
difference (m-w)		92	60	32
IRN-09v	marsh	31	153	-122
IRN-12v	water	-64	95	-159
difference (m-w)		95	58	37
IRN-09v	marsh	31	153	-122
IRN-11v	water	-39	105	-144
difference (m-w)		70	48	22
IRN-09v	marsh	31	153	-122
IRN-10v	water	-21	111	-132
difference (m-w)		52	42	10
Leeville study area: transect LEE-08 TO LEE-07 (fig. 12)				
LEE-08v	marsh	48	136	-88
LEE-09v	marsh edge	-29	84	-113
difference (m-w)		77	52	25
LEE-08v	marsh	48	136	-88
LEE-04v	water	-74	42	-116
difference (m-w)		122	94	28

Table 1. Adjusted core depths (thickness) and NAVD88 elevations for the base of the first marsh correlated between cores at Bayou Perot, Ironton, Leeville, Fourchon, and Caminada study areas. —Continued

Core ID	Core Location	Core Elevation (cm NAVD88)	Adjusted Depth (cm)	Adjusted Elevation (cm NAVD88)
LEE-11v	marsh	30	116	-86
LEE-03v	water	-43	51	-94
difference (m-w)		73	65	8
LEE-11v	marsh	30	116	-86
LEE-10v	marsh edge	-31	107	-138
difference (m-w)		61	9	52
LEE-11v	marsh	30	116	-86
LEE-05v	water	-61	90	-151
difference (m-w)		91	26	65
LEE-07B	marsh	33	170	-137
LEE-06v	water	-57	72	-129
difference (m-w)		90	98	-8
LEE-07B	marsh	33	170	-137
LEE-13v	marsh edge	-36	98	-134
difference (m-w)		69	72	-3
Fourchon study areas, transect FCN-01 TO FCN-09 (fig. 14)				
FCN-01p	marsh	42	119	-77
FCN-02v	marsh edge	3	94	-91
difference (m-w)		39	25	14
FCN-01p	marsh	42	119	-77
FCN-03v	water	-69	48	-117
difference (m-w)		111	71	40
FCN-01p	marsh	42	119	-77
FCN-04v	water	-58	97	-155
difference (m-w)		100	22	78
FCN-01p	marsh	42	119	-77
FCN-05v	water	-49	50	-99
difference (m-w)		91	69	22
FCN-08p	marsh	42	93	-51
FCN-05v	water	-49	50	-99
difference (m-w)		91	43	48
FCN-08p	marsh	42	93	-51
FCN-06v	water	-47	21	-68
difference (m-w)		89	72	17
FCN-08p	marsh	42	93	-51
FCN-07v	marsh edge	-16	52	-68
difference (m-w)		58	41	17

Table 1. Adjusted core depths (thickness) and NAVD88 elevations for the base of the first marsh correlated between cores at Bayou Perot, Ironton, Leeville, Fourchon, and Caminada study areas. —Continued

Core ID	Core Location	Core Elevation (cm NAVD88)	Adjusted Depth (cm)	Adjusted Elevation (cm NAVD88)
FCN-08p	marsh	42	93	-51
FCN-11v	water	-61	52	-113
difference (m-w)		103	41	62
FCN-09v	marsh	35	66	-31
FCN-11v	water	-61	52	-113
difference (m-w)		96	14	82
FCN-09v	marsh	35	66	-31
FCN-10v	marsh edge	-20	77	-97
difference (m-w)		55	-11	66
Caminada study area, transect CAM-09 to CAM-16 (fig. 16)				
CAM-09p	marsh	30	108	-78
CAM-10v	marsh edge	-37	49	-86
difference (m-w)		67	59	8
CAM-11p	marsh	40	131	-91
CAM-02v	water	-55	50	-105
difference (m-w)		95	81	14
CAM-15p	marsh	40	107	-67
CAM-16v	marsh edge	-7	62	-69
difference (m-w)		47	45	2
Caminada study area, transect CAM-04 to CAM-07 (fig. 17)				
CAM-04v	marsh	30	132	-102
CAM-14v	marsh edge	-19	81	-100
difference (m-w)		49	51	-2
CAM-04v	marsh	30	132	-102
CAM-05v	water	-51	54	-105
difference (m-w)		81	78	3
CAM-15p	marsh	40	107	-67
CAM-05v	water	-51	54	-105
difference (m-w)		91	53	38
CAM-15p	marsh	40	107	-67
CAM-08v	water	-29	63	-92
difference (m-w)		69	44	25
CAM-15p	marsh	40	107	-67
CAM-07v	water	-64	36	-100
difference (m-w)		104	71	33

[1]Uses marsh elevation at core site IRN-07 and assumes a minimum of 31 cm erosion between marsh core IRN-07p and marsh-edge core IRN-08v.

Table 2. Radiocarbon ages, carbon-isotope ratios, and calculated rates of sedimentation for selected organic samples at each of the study areas.

[Maximum and minimum calibrated ages were calculated using the program OxCal (Bronk Ramsey, 2001). See text for description of stratigraphic horizons. Abbreviations: F, fresh marsh; I, intermediate marsh; B, brackish marsh; S, saline marsh; cm, centimeters; B.P., before present; δ13C, carbon-isotope ratio; ‰, per mil; mm/yr; millimeters per year]

Core ID	Sample Depth (cm)	Stratigraphic Horizon	Conventional Age (B.P.)	Calibrated Age (B.P.)		δ13C (‰)	Paleo-Wetland Setting	Thickness (cm)	Composition (Unit)	Interval Rate (mm/yr)	Depth Rate (mm/yr)
				Max	Min						
Bayou Perot study area											
BP-02v	18-19	base of unit F	1230 ± 30	1261	1069	-23.05	I	18	peat + mud (E)	1.1	[1]0.2
BP-02v	37-38	top of unit D	1390 ± 35	1359	1267	-22.71	I	21.5	peat (D)	1.2	[1]0.3
BP-02v	57.5-58.5	base of unit D	1570 ± 30	1530	1394	-16.52	S	11.5	peat + mud (C)	1.2	[1]0.4
BP-02v	70-71	top of unit B	1670 ± 25	1689	1523	-25.05	F-I	62	peat (B)	0.9	[1]0.4
BP-02v	131-132	unit A	2360 ± 20	2457	2338	-26.41	F-I				0.6
BP-03v	77-78	top of unit F	1760 ± 30	1806	1567	-16.42	B	31	peat (F)	0.8	[1]0.4
BP-03v	107-108	base of unit F	2130 ± 30	2299	2001	-16.24	B	19	mud (E)	1.9	[1]0.5
BP-03v	127-128	top of unit D	2230 ± 30	2336	2153	-19.85	B				[1]0.6
BP-03v	151-152	base of unit D	2230 ± 25	2334	2154	-23.84	I				[1]0.7
BP-03v	154-155	base of unit D	2530 ± 30	2745	2491	-18.55	B				
BP-03v	164-165	top of unit B	2350 ± 30	2464	2330	-25.48	F	57	peat (A-B)	1.6	[1]0.7
BP-03v	220-221	base of unit A	2700 ± 40	2869	2749	-26.87	F				[1]0.8
BP-04v	111-112	top of unit D	1900 ± 30	1923	1737	-25.33	F-I				[1]0.6
BP-09p	143-144	base of unit I	545 ± 20	630	520	-26.99	F	97	peat + mud (F-G)	1	2.6
BP-09p	241-242	unit E	1470 ± 30	1405	1305	-23.59	I	66	peat + mud	0.8	1.6
BP-09p	306-307	base of unit B	2260 ± 30	2345	2157	-22.59	I	66	peat + mud (A)	1.3	1.4
BP-09p	372-373	base of unit A	2750 ± 25	2922	2778	-25.75	F				1.4
BP-13p	134-135	base of unit I	520 ± 25	622	510	-26.84	F	45	mud (G)	0.8	2.6
BP-13p	180-181	top of unit F	1090 ± 25	1058	938	-19.73	I				1.7
BP-13p	209-210	base of unit F	1780 ± 40	1820	1572	-22.91	I				
BP-13p	230-231	base of unit E	1590 ± 30	1540	1407	-21.73	I				1.5
BP-13p	231-232	unit E	1590 ± 25	1534	1411	-20.41	I	8	mud	0.4	1.5
BP-13p	240-241	top of unit D	1780 ± 30	1815	1614	-23.08	I	41	peat (D)	1.5	1.3
BP-13p	280-281	base of unit D	2050 ± 35	2115	1930	-25.45	F	8	mud (C)	0.6	1.4
BP-13p	289-290	top of unit B	2190 ± 35	2325	2120	-26.12	F	47	peat (B)	6.7	1.3
BP-13p	335-336	base of unit B	2260 ± 25	2344	2158	-27.16	F				1.5
BP-13p	342-343	top of unit A	2220 ± 30	2330	2152	-26.97	F	29	mud (A)	11	1.5
BP-13p	364-365	base of unit A	2530 ± 40	2748	2473	-27.34	F				1.4
Ironton study area											
IRN-13v	23-24	base of last marsh	525 ± 25	625	510	-25.83	F	53	mud	1.3	[1]0.5
IRN-13v	77-78	top of first marsh	920 ± 25	920	777	-27.69	F				[1]0.8
IRN-13v	118-119	base of first marsh	875 ± 25	905	728	-24.88	F				[1]1.4
IRN-15p	118-119	base of last marsh	575 ± 30	648	530	-26.37	F	24	mud	0.3	2.1
IRN-15p	143-144	top of first marsh	1270 ± 30	1286	1095	-27.2	F				1.1
Leeville study area											
LEE-08p	198-199	base of first marsh	490 ± 30	540	505	-25.72	F				4.1
Fourchon study area											
FCN-01p	113-114	base of first marsh	355 ± 30	498	316	-26.35	F				3.2
FCN-08p	89-90	base of first marsh	520 ± 30	626	507	-26.71	F				1.7
FCN-08p	91-92	base of first marsh	modern			-11.06	S				
Caminada study area											
CAM-02v	47-48	base of first marsh	630 ± 30	664	552	-24.14	I				[1]0.8

[1]Not true deposition rate due to erosion of uppermost marsh sediments.

Water-Level Measurements and Elevation Corrections

The water depth at each coring site and at points along transects between core locations was measured with a graduated rod, while the geographic coordinates of each depth measurement were obtained simultaneously with a GPS receiver. Water-level fluctuations at the coring sites during field operations were assumed to be comparable to those recorded at nearby tide gages (fig. 5 and Morton and others, 2003).

Water depths and marsh elevations measured in the field (table 1) can be compared only if they are corrected for any local conditions (tidal stage) that would influence the water-level data. The USGS and the Louisiana Department of Natural Resources (LDNR) operate independent networks of tide gages located throughout the coastal waters of south Louisiana. Using electronic tide-gage data from the USGS and LDNR websites, primary water levels and marsh elevations for the dates and times of data collection (fig. 5) were corrected to the North American Vertical Datum of 1988 (NAVD88). Water levels measured at Bayou Perot were corrected using data from a USGS tide gage (USGS #07380335) located about 10 kilometers (km) to the south in Little Lake; water levels measured at Ironton were corrected using data from a LDNR coastal monitoring station (#BA03C-61) located about 2 km to the south in Bayou Dupont; and water levels measured at Leeville, Fourchon, and Caminada were corrected using data from an interior-marsh USGS/LDNR Coastwide Reference Monitoring System (CRMS) site (CRMS #0164) located about 2 km northwest of the Caminada study area (fig. 1).

Core Deformation

The organic-sediment sections recovered in the push cores typically are thicker than those recovered by the vibracores. The thickness discrepancies are partly caused by the two different coring techniques. Vibracoring tends to compact the saturated sediments, making them seem thinner than they actually are. At most vibracoring sites, the core barrel penetrates deeper than the length of sediment that is recovered. When core-barrel penetration and recovered-sediment thickness are compared, it is assumed that all of the cored sediment is retained in the core barrel and none falls out the lower end when the core barrel is extracted. The difference between core-barrel penetration depth and recovered-sediment thickness is commonly reported as sediment compaction (appendix), although a more accurate definition of the difference is core shortening (Morton and White, 1997).

Core shortening is estimated in the field by measuring how far the surface of the sediment in the core barrel is below the actual sediment surface. After the core is opened, the stratigraphic intervals that are influenced by core shortening can be determined visually by identifying the zones of sediment disturbance (see core photographs in appendix). The degree of sediment deformation can be determined by comparing the stratigraphic contacts and laminae with actual or inferred horizontal planes across the core. The horizontal planes represent the expected configuration of undisturbed sediments. Some zones of disturbed sediments are also apparent because they occur between zones of undisturbed sediments (appendix, IRN-05Bv, 190 cm). Criteria for recognizing the zones of sediment disturbance and core shortening include bending of stratigraphic contacts as a result of frictional drag along the core barrel (appendix, LEE-08v below 140 cm and IRN-01v below 150 cm) and contortion of sediment laminae (appendix, CAM-05v, 90-200 cm and IRN-15v, 130 cm).

Core shortening is typically greatest when the bottom of the core barrel is plugged with stiff mud or a root mat. The zone of greatest sediment disturbance can be within or below the upper organic-rich marsh sediments. When shortening is concentrated below the organic-rich section, it is typically below the contact between the firm massive mud with relatively low water content and the underlying muddy sand or interlaminated mud with relatively high water content. The frictional resistance of the firm mud causes liquefaction of the water-saturated sediments, and core bypassing results as the firm mud pushes some of the liquefied sediments aside.

Core shortening is seldom addressed in published papers and when it is, the information presented is limited. An exception was the investigation of core sediment compaction by Kuecher (1994). After examining the physical properties and percent recovery relative to sample depth of sediments in a moderately deep push core taken in Terrebonne Parish, Kuecher (1994) concluded that most of the compaction occurred in the shallowest sediments; peats and organic clays were the sediment types most susceptible to compaction. From this, he developed an algorithm based on sediment type and sample depth to decompact the vibracores used in his investigation.

There are no standard quantitative definitions for the magnitudes of compaction. For the purposes of this report, core compaction is reported relative to total penetration and is defined as minor (0-10%), moderate (11-20%), or major (> 20%). Major compaction may preclude using the stratigraphic data for quantitative analysis, depending on which stratigraphic intervals are shortened.

Coring techniques, such as limiting initial penetration rates or sharpening the leading edge of the core barrel, can be adjusted to minimize compaction of the surficial organic-rich section. Despite efforts to minimize compaction, some marsh sediments may be compacted enough to influence the magnitudes of subsidence estimated from stratigraphic correlation of core pairs. Because imprecision may be introduced by facies changes at the basal organic-clastic contact and (or) by core shortening, results of stratigraphic comparisons should be viewed as providing approximate magnitudes of subsidence and erosion (table 1) and a way of determining relative significance of the two processes in converting former wetlands to open water. The subsidence and erosion estimates should not be viewed as absolute, highly accurate values.

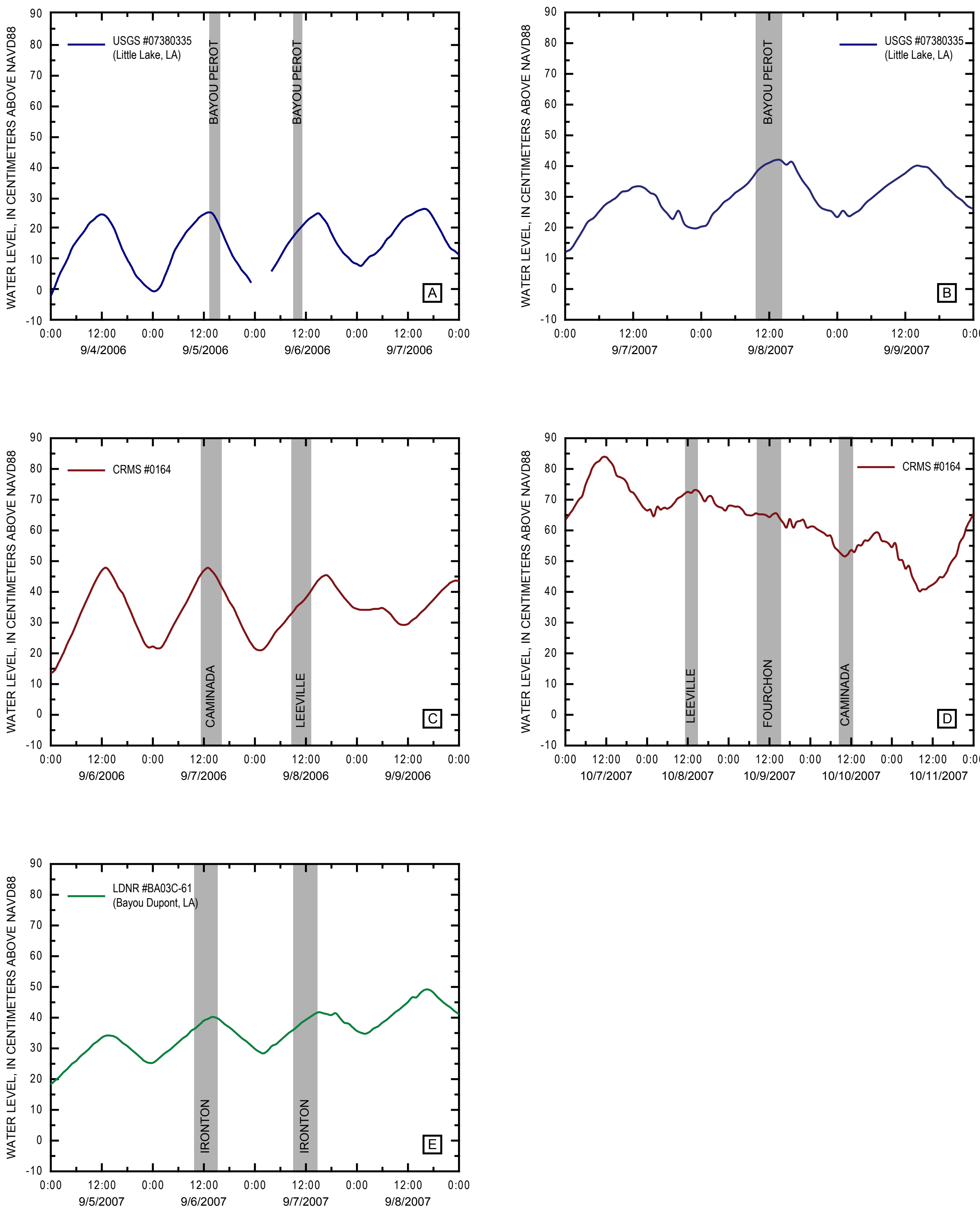

Figure 5. Water levels recorded at U.S. Geological Survey (USGS) site #07380335 (Little Lake, LA) on (A) September 4-7, 2006 and (B) September 7-9, 2007, Coastwide Reference Monitoring System (CRMS) site #0164 on (C) September 6-9, 2006 and (D) October 7-11, 2007, and (E) Louisiana Department of Natural Resources (LDNR) site #BA03C-61 (Bayou Dupont, LA) on September 5-8, 2007. Phases of the tides during field operations are highlighted (in gray). Gage locations are shown in figure 1.

Isotopic Analyses

Peat samples from selected cores were submitted to the National Ocean Sciences Accelerator Mass Spectrometry (AMS) Facility at the Woods Hole Oceanographic Institution for isotopic analysis of the organic material. The laboratory provided radiocarbon ages (^{14}C) and corresponding carbon-isotope ($\delta^{13}C$) values for the remains of former delta-plain marsh plants (table 2). Chmura and others (1987) conducted a statistical analysis of $\delta^{13}C$ ratios for extant plants comprising the fresh, intermediate, brackish, and saline marshes of the Barataria basin of the Mississippi delta. The ranges and means of $\delta^{13}C$ ratios for these marshes (table 3) were used to interpret the ecological setting of marshes preserved in the study cores.

The radiocarbon analyses produced four chronostratigraphic reversals whereby older dates occur above younger dates (table 2). Each of the reversals occurs where mud separates the sampled peats. Two of the anomalous older dates (BP-13p at 335-336 cm and IRN-13v at 077-078 cm) fall within the overlapping envelope of error with the underlying younger dates; therefore, they are considered to be essentially the same age. The other two anomalies (BP-13p at 209-210 cm and BP-3v at 154-155 cm) are about 200 years (yr) older than the underlying dates, and these discrepancies remain unexplained.

Average long-term geological rates of delta-plain subsidence can be inferred from burial histories of peats, using the peat depths below the surface and the ^{14}C peat ages (Penland and others, 1988; Roberts and others, 1994; Kulp and Howell, 1998). Results of comparable calculations (table 2) can also be expressed as average long-term geological rates of sediment aggradation. For this report, peat-burial histories are expressed as subsidence rates rather than sediment-aggradation rates. For cores with more than one dated peat, two different inferred subsidence rates can be calculated using the same data. Taking the peat depth and dividing by its age gives the simplest but least precise estimate. This depth-rate calculation yields an overall average rate of subsidence, which can be substantially influenced by high or low sedimentation rates above the dated peat. Missing section above the dated peat, which can occur because of erosion, can also significantly reduce the calculated rate of sedimentation (table 2, cores BP-02v and BP-03v). A more precise method recognizes that different rates of subsidence can occur at different times. For the second method, the difference in depths and difference in peat ages at the top and bottom of an interval are used to calculate the interval-specific subsidence rate. This method of differences restricts the averaging to only the interval of interest. Where possible, subsidence rates for both depth-rate and interval-rate methods were calculated (table 2).

Table 3. Ranges and means of $\delta^{13}C$ measured in plants from marshes in Barataria basin, Louisiana.

[‰, per mil; from Chmura and others (1987)]

Marsh Type	Range (‰)	Mean (‰)
Fresh	27.4 – 28.4	27.8
Intermediate	18.4 – 25.0	22.1
Brackish	15.3 – 20.4	16.9
Saline	14.4 – 17.7	16.2

Sedimentary Facies and Depositional History

Sediment Descriptions

Most of the cores recovered a succession of unconsolidated sediments representing three general sedimentary facies. The most common facies, from youngest to oldest, are: (1) an organic-rich section consisting of roots, peat, and interbedded organic-rich mud, (2) massive mud or clay, and (3) interlaminated mud. At the emergent-marsh sites, the youngest sediments consist of a mat of large fibrous roots interspersed with water-saturated gray or brown mud associated with living *Spartina* sp. marsh plants. The “live” roots and saturated mud indicate recent accumulation of both organic and clastic sediments. Below the most recent marsh deposits are black peat deposits with abundant fibrous roots that contain some dispersed mud. In most of the cores, peat and organic-rich sediments are in gradational contact with, or alternate with, thin beds of mud that contain roots or root traces. The organic content of the sediments (appendix) was estimated visually, not analytically.

The second sedimentary facies is an olive-gray mud or clay that typically contains abundant root traces. The root traces and total organic content decrease with depth. The massive appearance of this facies is likely the result of extensive bioturbation. The massive mud is gradational with the underlying interlaminated facies. The deepest facies penetrated by most vibracores consists of interlaminated mud and silt or mud and muddy sand. In some cores, these alternating layers are distinct and the contacts are horizontal, which indicates that this part of the core is undisturbed. Some of the deepest cores at the Ironton and Fourchon study areas encountered muddy sediments containing abundant oyster shells, indicating a former mixed-salinity open-water estuary.

Mud Accumulation and Probable Causes

Mud partings in the organic-rich sediments are more common in middle and upper delta-plain settings, such as at Bayou Perot and Ironton, than in lower delta-plain settings, such as at Leeville, Fourchon, and Caminada, where the accumulation of peat at most coring sites was essentially uninterrupted. Considering the geological conditions at Bayou Perot and Ironton, prolonged periods of organic accumulation punctuated by periods of clastic invasion may have been caused by two different physical processes: (1) episodic overbank flooding of a distributary channel associated with storm events or seasonal flooding and (or) (2) periodic submergence of the delta plain. Analytical errors associated with each radiocarbon date (± 20-40 yr) prevent determining the precise timing or duration of geological events. Nevertheless, the dates are adequate for determining the relative elapsed time for deposition of the mud layers. The duration of clastic-sediment accumulation that separated periods of organic-sediment accumulation may provide information about the processes involved. For example, overbank flooding would likely produce only a brief interruption of organic production because the rate of clastic sedimentation would be extremely rapid. The elevation of the delta-plain surface would increase slightly and would be available for rapid recolonization by wetland plants. Most fluvial flooding events last only a few days to a week, which is well below the resolution of radiocarbon dating. Given the error range of the dates, floods would be recorded as essentially the same peat date before and after mud deposition. In contrast, mud deposition filling accommodation space created by submergence likely would be prolonged, and certainly slower than rapid emplacement by a flood. Therefore, mud intervals with dates spanning hundreds of years are probably the products of submergence rather than overbank flooding. The contacts between organic and clastic deposits also can indicate whether the change in sedimentation style was gradual or abrupt, which may provide clues to the predominant processes responsible for the organic-to-clastic changes.

At Bayou Perot, the organic-rich sediments representing the marsh delta-plain environment record a repeated history of marsh construction and aggradation followed by periods of marsh inundation and deposition of mud. Peats that are 30 to 50 cm thick represent the periods of stable wetland production and accumulation of organics, whereas layers of gray mud, interbedded mud and peat, or organic-rich mud represent periods of inundation and significant influx and preservation of clastic sediments. The lithostratigraphic and chronostratigraphic evidence indicates episodes of both flooding and submergence. An example of rapid sedimentation likely associated with distributary flooding is the 6 cm of clay in BP-13p between 336 cm and 342 cm with essentially the same dates above and below the mud. However, lower contacts of most of the muddy units (C, E, G) are gradational, and the rates of deposition are low (table 2), which implies relatively slow periods of submergence and mud deposition.

At Ironton, the first (oldest) marsh formed about 875 yr ago (table 2). A single, discontinuous layer of organic-rich mud of variable thickness divides the peat section. Sedimentation rates for the first marsh and intervening mud were relatively high (table 2), probably because Ironton is located on the western margin of the Mississippi River. At Ironton, the contact between the mud parting and underlying basal peat is gradual near its stratigraphic pinch-out and abrupt elsewhere. The sedimentation rates and freshwater ecological signatures indicate that the mud was probably deposited because of submergence but was still strongly influenced by fluvial input.

Ecological Settings

The radiocarbon dates and $\delta^{13}C$ values (table 2) establish the timing and ecological settings for wetland development at each coring site. The most complete history is for Bayou Perot, where the first wetlands, which developed about 2700 years before present (B.P.), were freshwater marshes. The freshwater marshes persisted despite periodic flooding and burial by mud. Between about 2300 and 1100 B.P., salinities increased slightly and the depositional setting shifted to an intermediate- or brackish-marsh environment. The brackish marshes also persisted despite periodic burial by mud. Between 1100 and 550 B.P., the depositional setting returned to a freshwater environment that has persisted to the present. The radiocarbon dates and $\delta^{13}C$ values delineate age and salinity gradients between cores BP-13p and BP-3v. Correlative marshes at the BP-3v site tend to be older than marshes at BP-13p or BP-2v and BP-09p, but the salinity gradient generally increases between BP-13p and BP-2v (table 2).

Although data for the other coring sites are limited, trends can still be established. For example, all the peats sampled at Ironton were from freshwater marshes. In addition, the first marshes at Ironton and Leeville were freshwater types, but those at Caminada and Fourchon were intermediate and saline, respectively.

Historical Subsidence and Erosion of Delta-Plain Marshes

The differential subsidence and erosion of the marsh surface within the interior marshes can be estimated by comparing elevations and vertical offsets of stratigraphic contacts that are correlated between adjacent cores along a transect (table 1). This method assumes that marsh-sediment thicknesses and stratigraphic positions of correlation markers are uniform over short horizontal distances (tens to hundreds of meters). The amount of erosion at the open-water core site is equal to the difference in marsh-sediment thickness between the open-water core and the adjacent marsh core. The amount of subsidence at the open-water core site is equal to the elevation difference between the correlated stratigraphic marker between the two adjacent cores. The estimates of subsidence and erosion at a core location equal the accommodation space created by the land-water change, which is the difference between the former marsh elevation and the existing water depth. Multiple methods are available for estimating magnitudes of land-surface erosion and subsidence when the marsh-sediment thicknesses in land cores are variable and the marsh sediments in either the land or open-water cores have apparently been compacted.

Marsh-sediment thickness in each land core. – This default method (Morton and others, 2003; 2005) is used to determine magnitudes of subsidence and erosion unless there is clear evidence that an alternative method should be used. The method assumes that compaction is not in the marsh-sediment section and the marsh-sediment thicknesses in land cores accurately represent true marsh-sediment thicknesses. If marsh sediments in the land cores are compacted relative to marsh sediments in the open-water cores, then subsidence will be overestimated and erosion will be underestimated by the amount of core shortening in the marsh-sediment section. When marsh sediments in open-water cores are compacted with respect to marsh sediments in the land cores, then subsidence will be underestimated and erosion will be overestimated by the amount of core shortening in the marsh-sediment section.

Averaging marsh-sediment thicknesses. – This method assumes that the average of marsh-sediment thicknesses in several cores is a better estimator of true marsh-sediment thickness at all sites than individual measurements or than the marsh-sediment thickness in the least-compacted core. The influence of this technique on the subsidence and erosion estimates depends on how close the average marsh-sediment thickness is to the true marsh-sediment thickness for each adjusted core.

Thickest or least-compacted marsh-sediment section in land cores. – This method assumes that the thickest or least-compacted marsh-sediment section is accurate and is representative of a uniformly thick deposit over a large area. It does not take into account natural variability in marsh-sediment thicknesses. However, a single core with the least-compacted marsh-sediment section could be highly compacted, leading to overestimation of subsidence. Conversely, a single core with a naturally thick, but unrepresentative, peat section could lead to underestimation of subsidence.

Linear adjustment of each compacted core. – This method assumes that core shortening is uniformly distributed throughout the core and that a decompacted thickness for the marsh-sediment section is a better estimator of the true marsh-sediment thickness than an unadjusted measurement is. The magnitude of influence on the subsidence and erosion estimates depends on how close the adjusted marsh-sediment thickness is to the true marsh-sediment thickness. This is the method most commonly used to adjust the measurements for compacted cores.

Interval adjustment of each compacted core. – This is the preferred method of adjusting shortened cores if accurate measurements are available for the shortened intervals. The method recognizes that core shortening is not uniform throughout the core and is typically concentrated in certain stratigraphic intervals because of contrasts in sediment physical properties. The method requires (1) interval correlation using a single standard core or a composite from several cores with intervals of true stratigraphic thickness and interval reconstruction for the shortened core or (2) multiple measurements of compaction with depth of coring (Morton and White, 1997). The interval-adjustment technique is seldom used because core-compaction estimates typically are single measurements taken after the core has reached its greatest penetration.

All of these techniques provide a minimum estimate of total land-surface subsidence because there is no measurement of the absolute amount of historical subsidence of the marsh surface relative to some standard vertical datum. The total amount of historical subsidence of the marsh sediments of the southeastern Mississippi delta plain is largely unknown.

Bayou Perot

The Bayou Perot study area is located in a middle-to-upper delta-plain interdistributary region between the modern Mississippi River and Bayou Lafourche (fig. 3). The latter channel was the primary distributary responsible for constructing the late Holocene Lafourche subdelta. In the interdistributary setting, marshes are composed typically of plants that thrive in brackish to freshwater. The marshes surrounding Bayou Perot and Bayou Rigolettes are dominated by the brackish- and intermediate-marsh species *Spartina patens* (Hymel, 2003; Reed, 1995). Although O'Neil (1949) mapped the Bayou Perot and Bayou Rigolettes area as brackish floating marsh, Swarzenski and others (1991) and Sasser and others (1996) reported that maximum vertical movement of the marsh mat was 3 cm in response to an approximately 45-cm fluctuation in water level at their study site southeast of Bayou Rigolettes. Consequently, they classified the marsh at Bayou Perot as non-floating "quaking" brackish marsh, indicating a condition transitional between floating marsh and fast-land marsh.

An 1891 topographic map shows Bayou Perot and Bayou Rigolettes as small meandering channels connecting Lake Salvador and Little Lake. Thus, tidal and meteorological forces have driven water continuously through Bayou Perot between these large open-water bodies for at least the last 100 years. The 1932-2006 land-water trends (Barras and others, 2008; John Barras, personal commun., 2008) show that most of the historic land loss near Bayou Perot and Bayou Rigolettes occurred along the shorelines of these water bodies as the channels enlarged (figs. 3 and 6). The greatest land loss occurred before 1978, but significant shoreline retreat has continued on both sides of Bayou Perot. Some historic interior ponding and marsh fragmentation occurred between the bayous and southeast of Bayou Rigolettes, but interior loss west of Bayou Perot was minor and mostly restricted to direct loss associated with construction of canals and pipelines. Historical wetland loss on the margins of Bayou Perot and Bayou Rigolettes was so great that the peninsula separating these water bodies was a candidate site for marsh restoration. However, the project plan was deauthorized in 1998 because the rate of bank retreat was extremely high (up to 35 m/yr; Hymel, 2003). Because of these high erosion rates, construction of shoreline protection structures designed to block wave energy and to prevent further marsh loss within the middle Barataria basin "landbridge" began in 2001. In the coring area, a concrete sheet-pile structure was constructed along the west side of Bayou Perot in the summer of 2007.

Wetland loss along the shores of Bayou Perot and Bayou Rigolettes has significantly enlarged their areas, and the margins of these channels have retreated systematically regardless of shoreline orientation with respect to wave impacts. However, it was unclear if the shoreline retreat was caused by wave and current erosion of the banks, submergence and retreat associated with land-surface subsidence, or a combination of both processes. The hydrologic setting of Bayou Perot and Bayou Rigolettes prompted Penland and others (2000) to classify the land loss around their margins as erosion by channel flow.

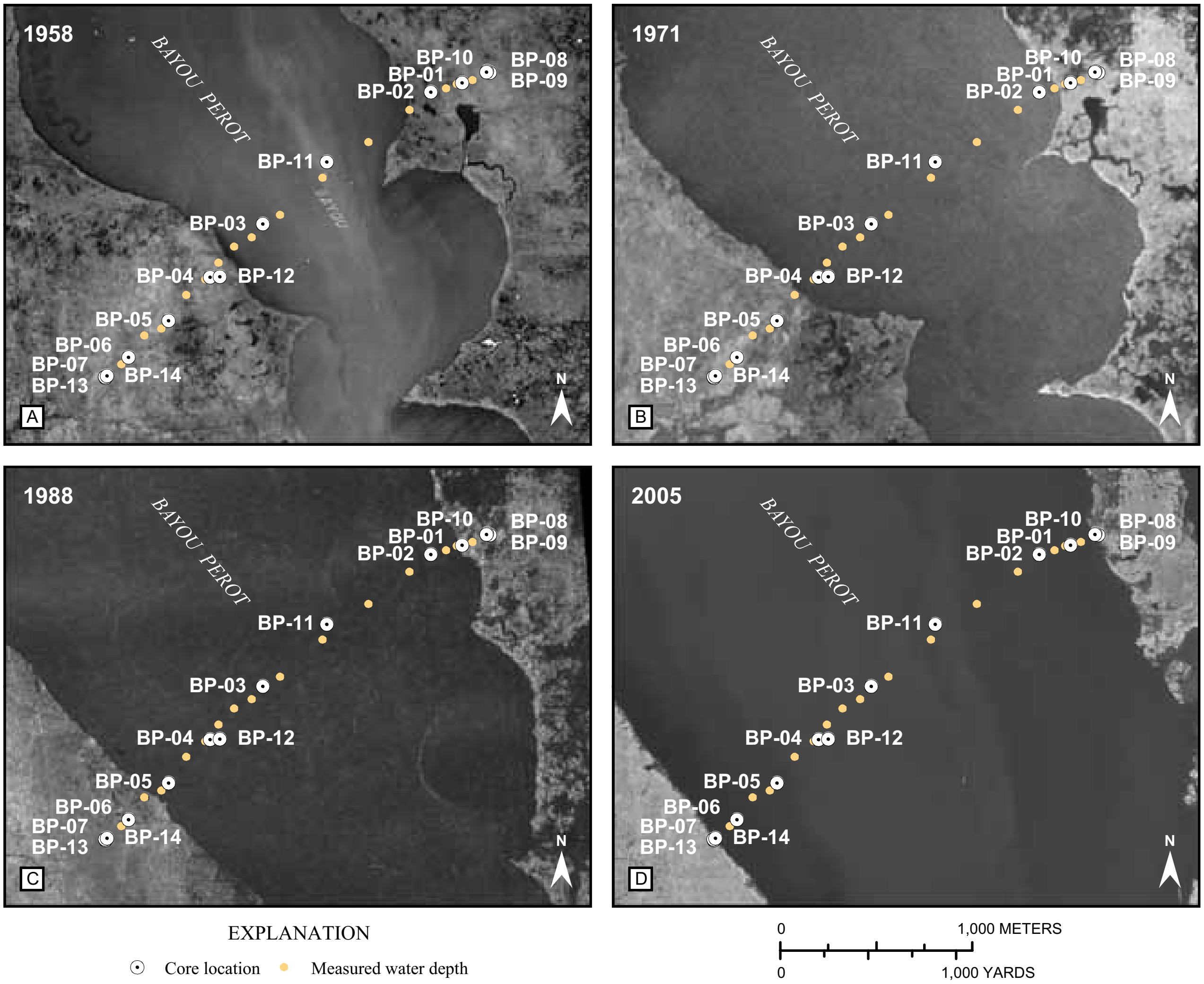

Figure 6. Locations of sediment cores and sediment-surface profiles from the Bayou Perot area superimposed on pre- and post-subsidence aerial photographs taken in (A) 1958, (B) 1971, (C) 1988, and (D) 2005. Image sources are (A) Edgar Tobin Aerial Surveys controlled aerial mosaic for Bayou L'Ours quadrangle, source imagery acquired May and October 1958; (B) U.S. Geological Survey (USGS) black-and-white aerial photography acquired October 11, 1971; (C) National Aeronautics and Space Administration (NASA) color-infrared (CIR) aerial photography acquired November 7, 1988; and (D) USGS Digital Orthophoto Quarter Quadrangle (DOQQ) for northeast quadrant of Bay L'Ours quadrangle, source imagery acquired November 18, 2005.

Bayou Perot was selected for investigating historical land-water changes and for testing the bank-erosion hypothesis. This was accomplished by collecting 17 shallow cores across Bayou Perot along a transect that intersected zones of sequential historical land loss on both sides of the bayou (figs. 3 and 6). Core BP-11v (fig. 6) was taken at a site that seemed to have been open water from at least the 1930s, prior to onset of rapid wetland loss. Compaction at Bayou Perot was minor in 5 out of 15 vibracores and moderate in 1 vibracore, but compaction was more than 20 percent in 9 vibracores taken in both marsh and open-water settings. Consequently, most of the cores at Bayou Perot underwent major compaction. The linear decompaction method was used to adjust sediment-contact depths and elevations for the purpose of estimating magnitudes of subsidence and erosion.

Marsh elevations are about 31 cm (core site BP-13) and 51 cm (core site BP-09) on the west and east banks of Bayou Perot, respectively (fig. 7). Water depths range from -11 to -219 cm and average about -135 cm where the marsh surface previously existed. Water depths drop off steeply from the marsh edge, exceeding -100 cm within 100 m from the shoreline. Although the deepest water within Bayou Perot (-219 cm) coincides with the historical position of the stream course, it is only about 30 cm deeper than adjacent water depths that were former marsh sites. Water depths progressively increase toward the former channel position, coinciding with the zones of sequential historical land loss (compare figs. 3 and 7).

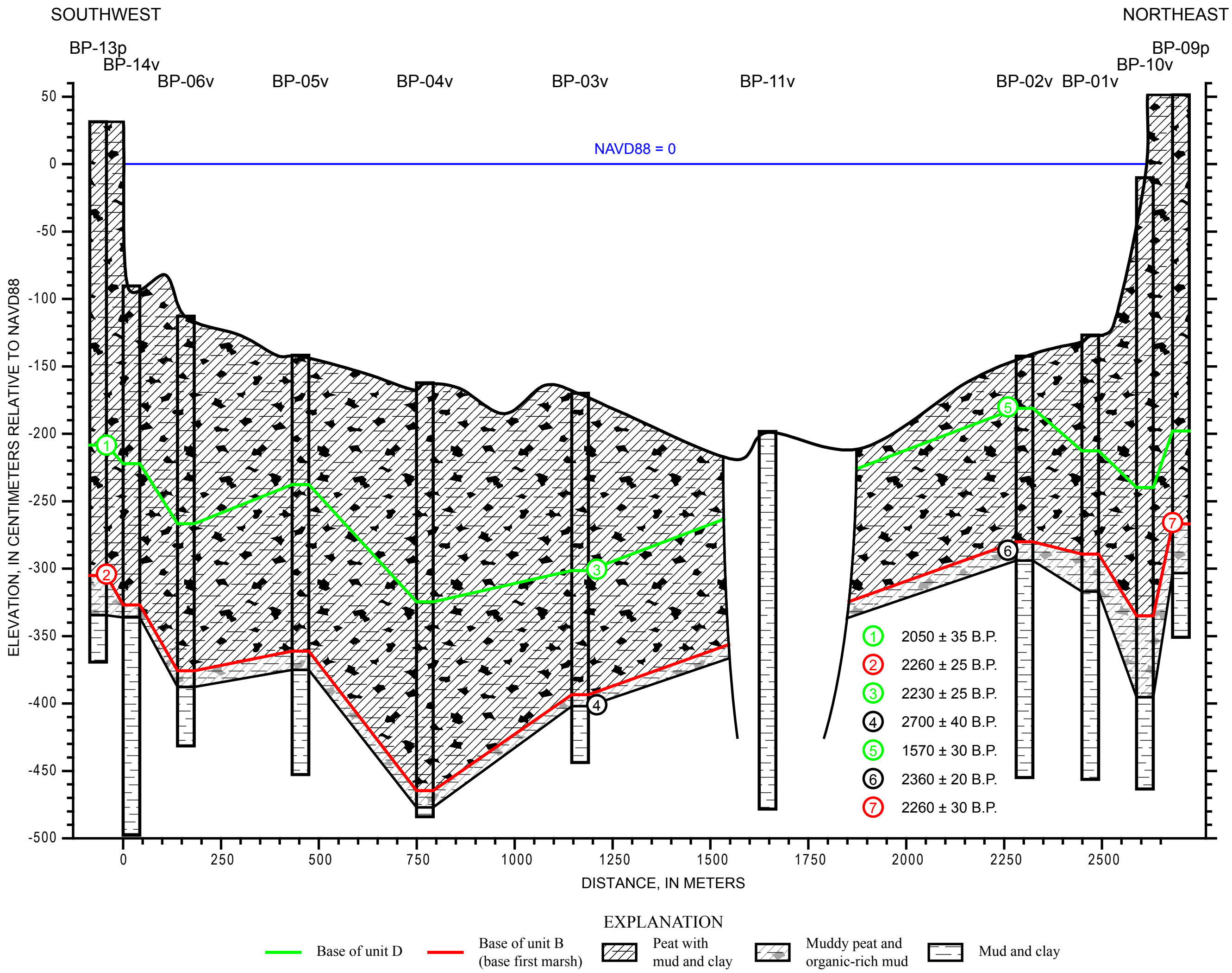

Figure 7. Combined bathymetric profile and stratigraphic cross section for marsh and open-water cores BP-13p to BP-09p illustrating the magnitude of subsidence and wetland erosion (in centimeters) at the Bayou Perot study area. Highlighted contacts are the top of unit D (in green) and the base of unit B (in red); associated radiocarbon ages are from table 2. Core locations are shown in figure 6; vertical scale is greatly exaggerated.

At Bayou Perot, the organic-rich section of the delta plain consists of relatively thick peat layers separated by relatively thin mud layers, or layers of alternating mud and organic-rich mud. The organic-rich section is thicker at Bayou Perot than at any of the other Barataria basin study areas. The subdivided units of the organic-rich section were assigned ascending letters, from oldest to youngest, to provide a basis for stratigraphic correlation (appendix, table 2). Unit A, which is a massive organic-rich mud that contains roots and thin peats, represents the transitional phase of delta-plain deposition prior to establishment of the first extensive marsh. Units B, D, and F are composed of peat with no mud, or very little interspersed mud or mud partings. Units C, E, and G are composed of thin alternating mud and organic-rich mud layers that together present a banded appearance. Beneath the youngest root-mat and peat unit is an inclined contact (I). This contact marks the base of the modern delta-plain marsh and its transition with the underlying mud. Stratigraphic correlations among the Bayou Perot cores indicate that much of the compaction is in the youngest unit of root mat and peat.

Core BP-11v did not contain any of the organic-rich sediments like those contained in the other cores because it penetrated channel-fill deposits associated with the original waterway of Bayou Perot. Sediment compaction was greatest in BP-11v (134 cm), which indicates that some muddy sediments are as susceptible to compaction as are root-mat and peaty sediments. The channel-fill deposits are composed of homogeneous mud that contains articulated *Rangia cuneata* and *Rangia flexuosa* in growth position (appendix). These bivalves attest to the freshwater ecological conditions that persisted during the accumulation of upper delta-plain mud.

The open water at core BP-12v is underlain by interlaminated mud containing *Rangia* shells that overlies a section of organic-rich sediments. Stratigraphic correlations with other cores indicates that the shallow interlaminated mud represents relatively recent estuarine deposition subsequent to erosion of marsh sediments that are slightly younger than unit G. Isotopic dating would be necessary to determine precisely when the recent scour and fill occurred.

Cores BP-09p, BP-13p, and BP-03v (fig. 7 and appendix) served as the standards for correlating stratigraphic contacts and estimating magnitudes of erosion and subsidence at Bayou Perot. BP-09p and BP-13p are marsh push cores that should be minimally deformed and should accurately represent the composition and thickness of the stratigraphic units. Core BP-03v also is critical for stratigraphic correlation because it contains the three predominant alternating mud and peat units (C, E, G), it is in the transect middle, and the amount of core shortening is minor (11 cm, or 4 percent).

Unit B, the first marsh sequence at Bayou Perot, is the deepest laterally continuous marsh unit present in all cores, and its base was used for erosion and subsidence calculations (table 1). Considering the base of unit B, estimated erosion ranged from 74 cm (BP-06v) to 181 cm (BP-02v). Estimated magnitudes of subsidence ranged from 13 cm (BP-02v) to 89 cm (BP-03v). The relatively low erosion (34 cm) and high subsidence (160 cm) estimates at BP-04v may be exaggerated because of the decompaction adjustment of the lower peat section.

Water depths are shallowest around the margins of Bayou Perot where the least erosion and subsidence occurred, and they are greatest where both erosion and subsidence were greatest. Most of the open water at former emergent-marsh sites is attributable to erosion of the organic-rich sediment section (table 1). However, the magnitudes of subsidence and erosion are markedly different on opposite sides of the bayou. Subsidence accounts for as much as 89 cm of marsh submergence on the western side, but less than about 25 cm on the eastern side. The difference in marsh elevations at core site BP-13 (31 cm) and BP-09 (51 cm) is likely a result of the greater historical subsidence on the west side of Bayou Perot, where core BP-13p has subsided 38 cm relative to core BP-09p.

Ironton

The Ironton study area encompasses a middle-to-upper delta-plain setting that lies west of the artificial levee system of the modern Mississippi River (fig. 3). The coring sites are bounded by Cheniere Traverse Bayou to the north and a series of manmade canals that were constructed by 1958 to the east. An expanse of mostly unfragmented interior marsh exists between the coring sites and Bayou Dupont to the southwest. Since the 1950s, when well-established freshwater wetland plants formed a continuous marsh across the area, the Ironton wetlands have become increasingly fragmented and more saline. By 1988, the study area consisted of primarily brackish marshes dominated by *Spartina patens* (Boshart, 1993).

Although Britsch and Dunbar (1996) documented some wetland loss at Ironton during three periods (1956-1974, 1974-1983, 1983-1990) and initial, rapid hotspot formation east-southeast of the coring sites had occurred by 1974, the most substantial loss in the coring area occurred after 1978 (fig. 3). During the 1980s, the Ironton marshes became increasingly fragmented. Comparing aerial photographs from 1958 to 2005 (fig. 8) shows that as late as 1988, partially submerged marsh was visible below the water surface. By the early 1990s (not shown in fig. 8), most of the formerly emergent marsh vegetation in the study area was permanently submerged. Ironton was selected to investigate these more recent land-water changes.

Marsh elevations at the Ironton coring sites range from about 23 to 31 cm (figs. 9 and 10). Water depths, which range from -8 to -61 cm and average about -50 cm, tend to increase toward the center of the open-water bodies. Water depths at Ironton also are relatively shallow compared to previously studied wetland-loss sites (Morton and others, 2005), possibly because of the relatively young age of the water bodies. Core shortening at Ironton was mostly minor (5 out of 16 vibracores) to moderate (9 vibracores). The linear decompaction method was used to adjust sediment-contact depths and elevations for estimating magnitudes of subsidence and erosion.

At Ironton, the generalized stratigraphic succession in most cores consists of four facies: (1) a muddy root mat and (or) peat, (2) organic-rich mud with some dispersed peat, (3) thick, massive to interlaminated mud, and (4) massive mud with shells concentrated near the base. The facies 1 root-mat and peaty sediments are thinner in cores on the north side of the area of wetland loss (cores IRN-05v through IRN-08v) compared to those toward the south (fig. 9). In the west-central and northern parts of the study area (core sites IRN-15 to IRN-04 and IRN-13 to IRN-08, respectively), an organic-rich mud of variable thickness divides the peat section into two periods of marsh development (figs. 9 and 10). Some of the deepest cores (IRN-02v, IRN-03v, IRN-08v, IRN-10v, and IRN-11v) encountered an older peat with interbedded organic-rich mud below facies 3 and 4.

Push cores IRN-01p, IRN-07p, IRN-09p, and IRN-15p have such thick organic-sediment sections (facies 1) that the basal contact with underlying massive mud is deeper than the linear-adjusted depths for the same contact in open-water cores. Consequently, the push cores cannot be used to estimate erosion and subsidence. The exaggerated organic-facies thicknesses in the push cores may be an artifact of the coring operation.

To obtain estimates of erosion and subsidence at Ironton, the decompacted basal first-marsh contacts (base of facies 1) in marsh vibracores IRN-01v, IRN-09v, and IRN-15v and marsh-edge vibracore IRN-08v were obtained using the linear adjustment method (table 1). Because no vibracore was recovered from marsh-core site IRN-07, the adjacent marsh-edge vibracore IRN-08v was used as the standard. In order to account for total erosion of the open-water cores relative to the marsh surface at core site IRN-07, it is assumed that the 31-cm elevation difference between the top of core IRN-08v (-8 cm) and the marsh surface at core site IRN-07 (23 cm) consists of facies 1 peat. Thus, in table 1, the elevation at core IRN-07p (23 cm) is used as a proxy for the top of the facies 1 peat, and the difference (31 cm) is added to the IRN-08v adjusted depth (65 cm) to obtain a total facies 1 thickness (96 cm).

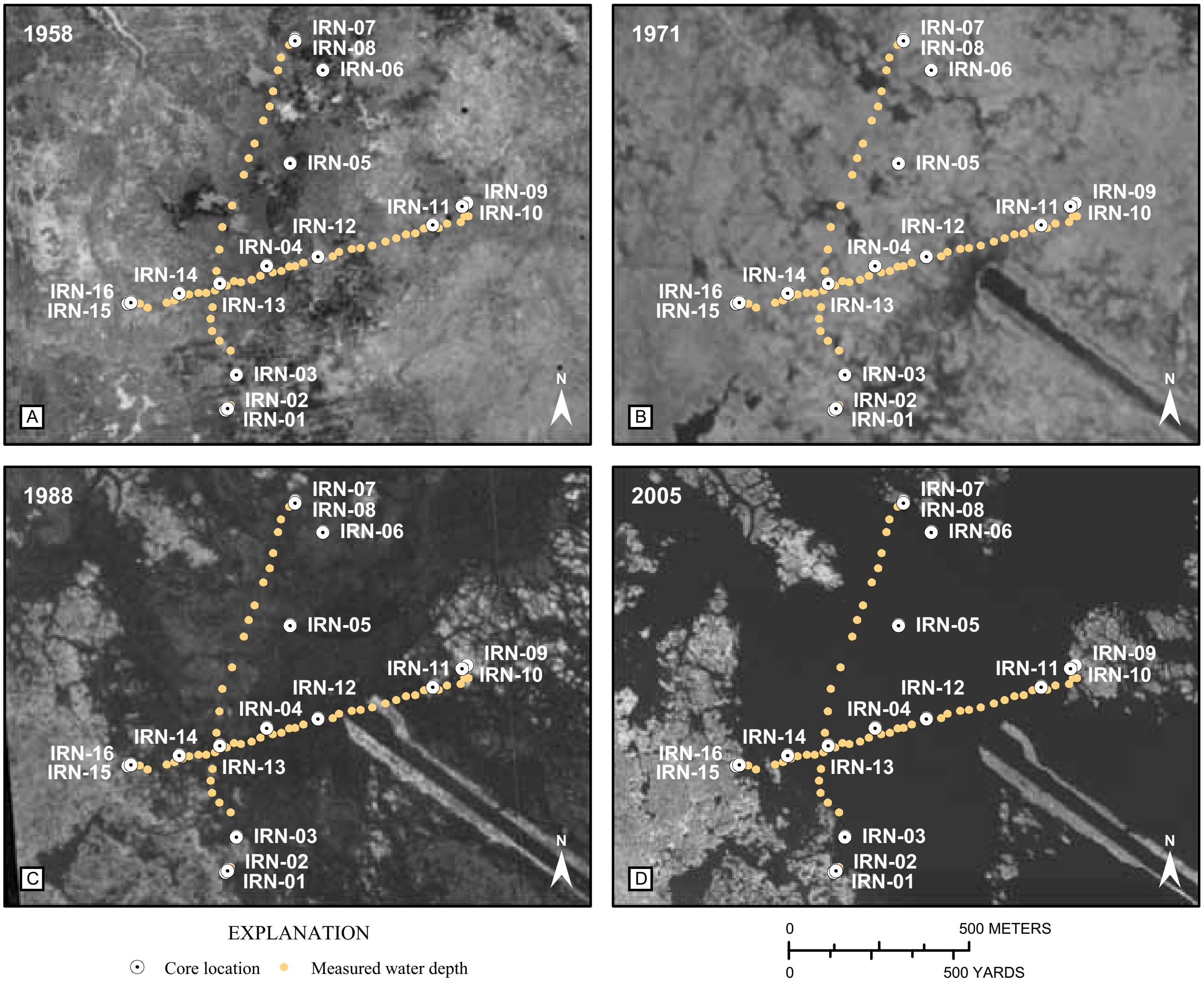

Figure 8. Locations of sediment cores and sediment-surface profiles from the Ironton area superimposed on pre- and post-subsidence aerial photographs taken in (A) 1958, (B) 1971, (C) 1988, and (D) 2005. Image sources are (A) Edgar Tobin Aerial Surveys controlled aerial mosaic for Lafitte quadrangle, source imagery acquired May and October 1958; (B) U.S. Geological Survey (USGS) black-and-white aerial photography acquired October 11, 1971; (C) National Aeronautics and Space Administration (NASA) color infrared (CIR) aerial photography acquired November 7, 1988; and (D) USGS Digital Orthophoto Quarter Quadrangle (DOQQ) for southeast quadrant of Lafitte quadrangle, source imagery acquired October 19, 2005.

The subsidence-erosion calculations indicate that erosion ranged from 13 cm (IRN-03v) to 77 cm (IRN-04v) and averaged about 45 cm, whereas subsidence ranged from 2 cm (IRN-16v) to 60 cm (IRN-03v) and averaged about 40 cm. Erosion was greater than subsidence at most of the open-water sites. Exceptions were at IRN-02v, IRN-03v, and IRN-13v, with the least compaction and a thick organic-rich mud interbedded within the facies 1 peat, and at IRN-05Bv and IRN-06v, where subsidence and erosion were about equal. Subsidence estimates at the first three core sites may be slightly exaggerated due to significant core shortening of the standard core IRN-01v.

For IRN-13v, the core common to both stratigraphic cross sections, the relative contribution of subsidence and erosion varies depending on which standard core is used for comparison. IRN-04v and IRN-12v are the two cores for which the accommodation space created by lowered marsh elevation and increased water depth is greatest and exceeds about 90 cm. In general, there is good agreement between the greatest estimated magnitudes of erosion and subsidence and corresponding depths of open water at former marsh sites.

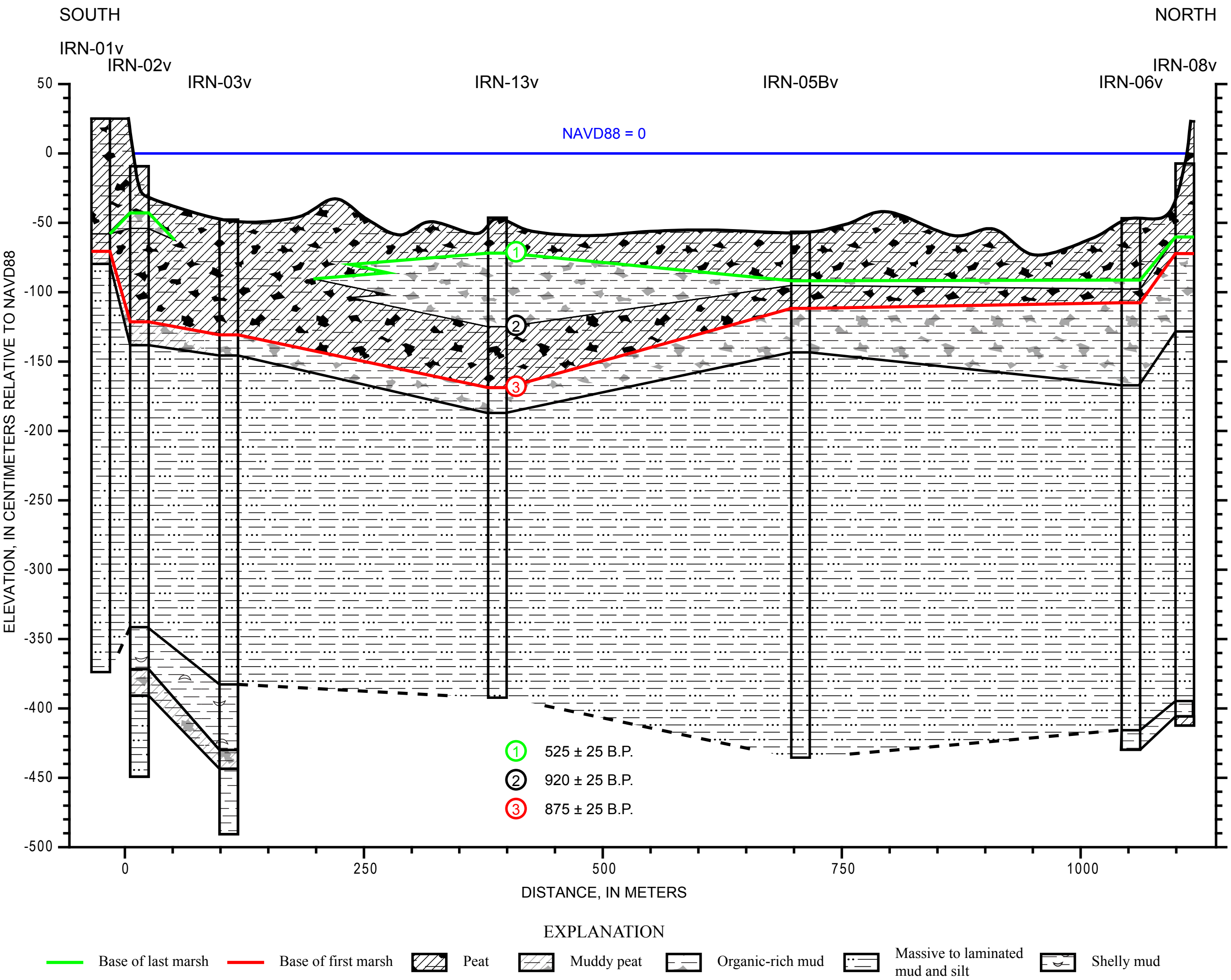

Figure 9. Combined bathymetric profile and stratigraphic cross section for marsh and open-water cores IRN-01v to IRN-08v illustrating the magnitude of subsidence and wetland erosion (in centimeters) at the Ironton study area. Highlighted contacts are the base of the last marsh (in green; where present) and the base of the first marsh (in red); associated radiocarbon ages are from table 2. Core locations are shown in figure 8; vertical scale is greatly exaggerated.

Leeville

The Leeville study area is located on the lower delta plain of the Lafourche subdelta on the eastern side of Bayou Lafourche near its bifurcation with Bayou Moreau (fig. 4). The coring sites were in an area of formerly continuous emergent marsh that now is mostly open water with a remnant fringe of emergent marsh. Most of the wetland conversion to open water in the Leeville study area occurred between 1978 and 1990, with some continued loss along the remaining marsh edges, especially at the southeast “apex” of the study area (adjacent to marsh-core site LEE-11). Comparing aerial photographs from 1958 to 2005 (fig. 11) shows that the 1978 landscape was very similar to the 1950s landscape when the marsh was continuous, although areas of partly submerged marsh are present under high-water conditions (not shown in fig. 11). The general pattern of wetland loss was established by 1989, and there was little change in land-water patterns after 1998. Marsh-core site LEE-07 is located along the southwestern shoreline of an unnamed interior pond that formed prior to, and has remained relatively stable since, the 1950s (figs. 4, 11).

Although there are no manmade canals between core locations, the Leeville study area is essentially bounded on all sides by canals, and there is a dense network of canals associated with the Leeville oil-and-gas field in marshes north and west of the coring sites. A small, south-trending, inactive distributary channel is visible between core sites LEE-03 and LEE-04 prior to 1989, approximately dividing the study area into western and eastern halves. William Canal, which forms the southern boundary of the study area, was constructed by 1952 (not shown in fig. 11), the north-south canal that bounds the study area to the east was constructed by 1958, and the present network of canals, including the southwest-northeast canal that bounds the study area to the north, was fully developed by 1978.

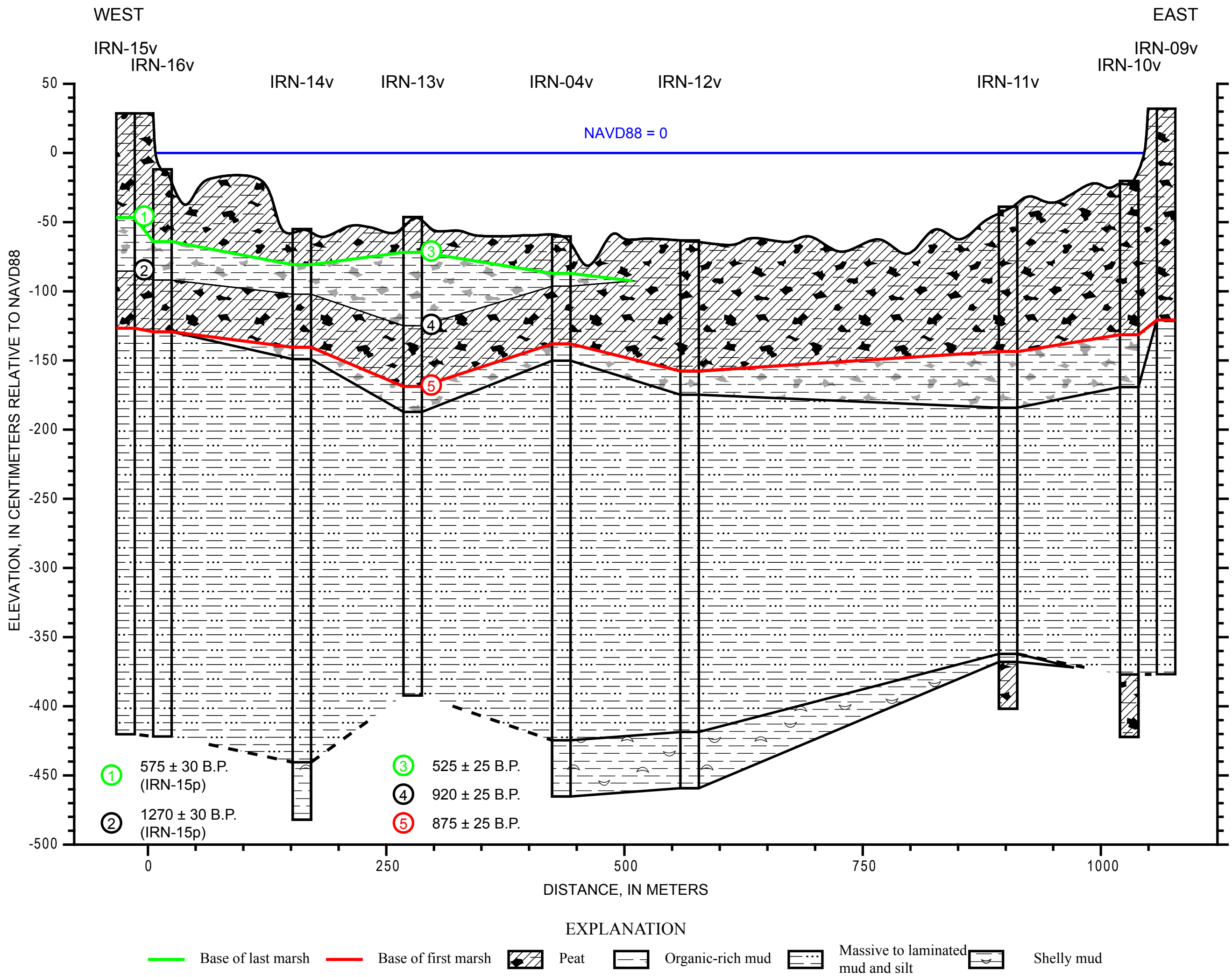

Figure 10. Combined bathymetric profile and stratigraphic cross section for marsh and open-water cores IRN-15v to IRN-09v illustrating the magnitude of subsidence and wetland erosion (in centimeters) at the Ironton study area. Highlighted contacts are the base of the last marsh (in green; where present) and the base of the first marsh (in red), and associated radiocarbon ages are from table 2. Core locations are shown in figure 8; vertical scale is greatly exaggerated.

At Leeville, marsh elevations range from 26 cm to 48 cm, and water depths range from -11 to -90 cm and average about -55 cm (fig. 12). Core shortening was mostly minor (3 out of 14 vibracores) to moderate (8 vibracores) but was major in 3 marsh vibracores (LEE-07Bv, LEE-08v, and LEE-12v). The linear decompaction method was used to adjust sediment-contact depths and elevations for the purpose of estimating magnitudes of subsidence and erosion.

The general stratigraphy at nearly all the Leeville coring sites consists of four predominant sedimentary facies: (1) peat with muddy peat or interbedded mud and peat at the base, (2) a thin, organic-rich mud, (3) massive mud and clay, and (4) a relatively thick section of interlaminated mud and silt with whole shells (*Rangia cuneata*) and shell fragments. A few cores penetrated a shell lag overlying massive mud below the interlaminated mud, and one core (LEE-09v) recovered some muddy sand below the lower massive mud.

Marsh push cores LEE-08p, LEE-11p, and LEE-12p have such thick organic-sediment sections that the basal contact with underlying massive mud is deeper than the linear-adjusted depths for the same contact in marsh-edge and open-water cores. Consequently, the push cores cannot be used to estimate erosion and subsidence. To estimate erosion and subsidence at Leeville, depths of the decompacted base of facies 1, which represents the first widespread marsh development, in marsh vibracores LEE-08v, LEE-11v, and LEE-07Bv were calculated using the linear adjustment method (table 1).

The accommodation space formed at Leeville as a result of conversion of wetlands to open water ranged from 61 to 122 cm and averaged about 85 cm. Marsh-sediment erosion ranged from 9 to 97 cm and subsidence ranged from essentially zero to 65 cm. The predominance of one process over the other was constrained spatially with erosion exceeding subsidence in the western and eastern areas, whereas subsidence exceeded erosion only in the southern area at LEE-05v and LEE-10v (fig. 12).

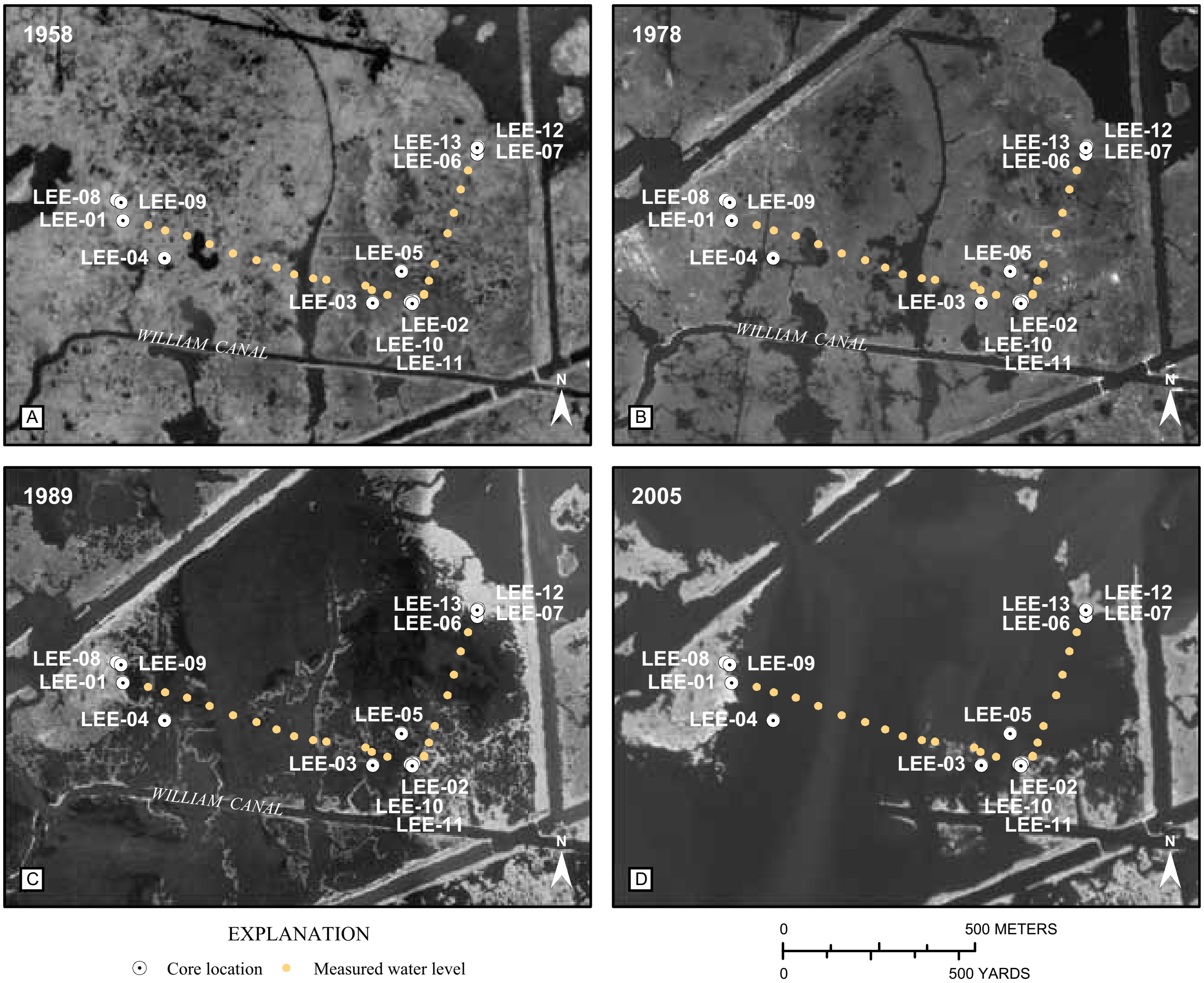

Figure 11. Locations of sediment cores and sediment-surface profiles from the Leeville study area superimposed on pre- and post-subsidence aerial photographs taken in (A) 1958, (B) 1978, (C) 1989, and (D) 2005. Image sources are (A) Edgar Tobin Aerial Surveys controlled aerial mosaic for Leeville quadrangle, source imagery acquired October, 1958; (B) U.S. Geological Survey (USGS) black-and-white aerial photography acquired March 27, 1978; (C) and (D) USGS DOQQs for northwest and northeast quadrants of Leeville quadrangle, source imagery acquired November 18, 2005.

Fourchon

The Fourchon study area is on the lower delta plain of the Lafourche subdelta, south of the bifurcation of Bayou Lafourche and Bayou Moreau and between the low natural levees that border those two distributary channels (fig. 4). Comparison of historical images shows that cores were taken where the marsh surface was nearly continuous in the early 1950s, except near core site FCN-11, which is located in a water body that formed between 1932 and 1956 (figs. 4 and 13). Marsh disintegration continued from the late 1950s through the late 1970s, but conversion of marsh to open water accelerated in the 1980s. By 1989, the landscape was very similar to the present landscape, and little or no subsequent land loss occurred after 1998 (not shown in fig.13). The Fourchon study area was selected for investigation because of its interdistributary setting and because much of the wetland loss there occurred later than major interior loss elsewhere in the delta plain.

Marsh elevations at Fourchon range from 35 to 42 cm, whereas water depths range from only a few centimeters to -69 cm and average about -50 cm (fig. 14). Water depths are slightly deeper on the western side of the core transect and where permanent water has persisted around core site FCN-11 since at least the 1950s (fig. 13).

Core shortening at Fourchon was highly variable with nearly equal numbers of cores undergoing minor (3 out of 12 vibracores), moderate (4 vibracores), and major compaction (5 vibracores). Compaction was greatest in the marsh and marsh-edge cores. As a result of the moderate to major compaction, the organic-clastic contacts in many cores are abrupt and some are deformed (FCN-04v, FCN-08v,

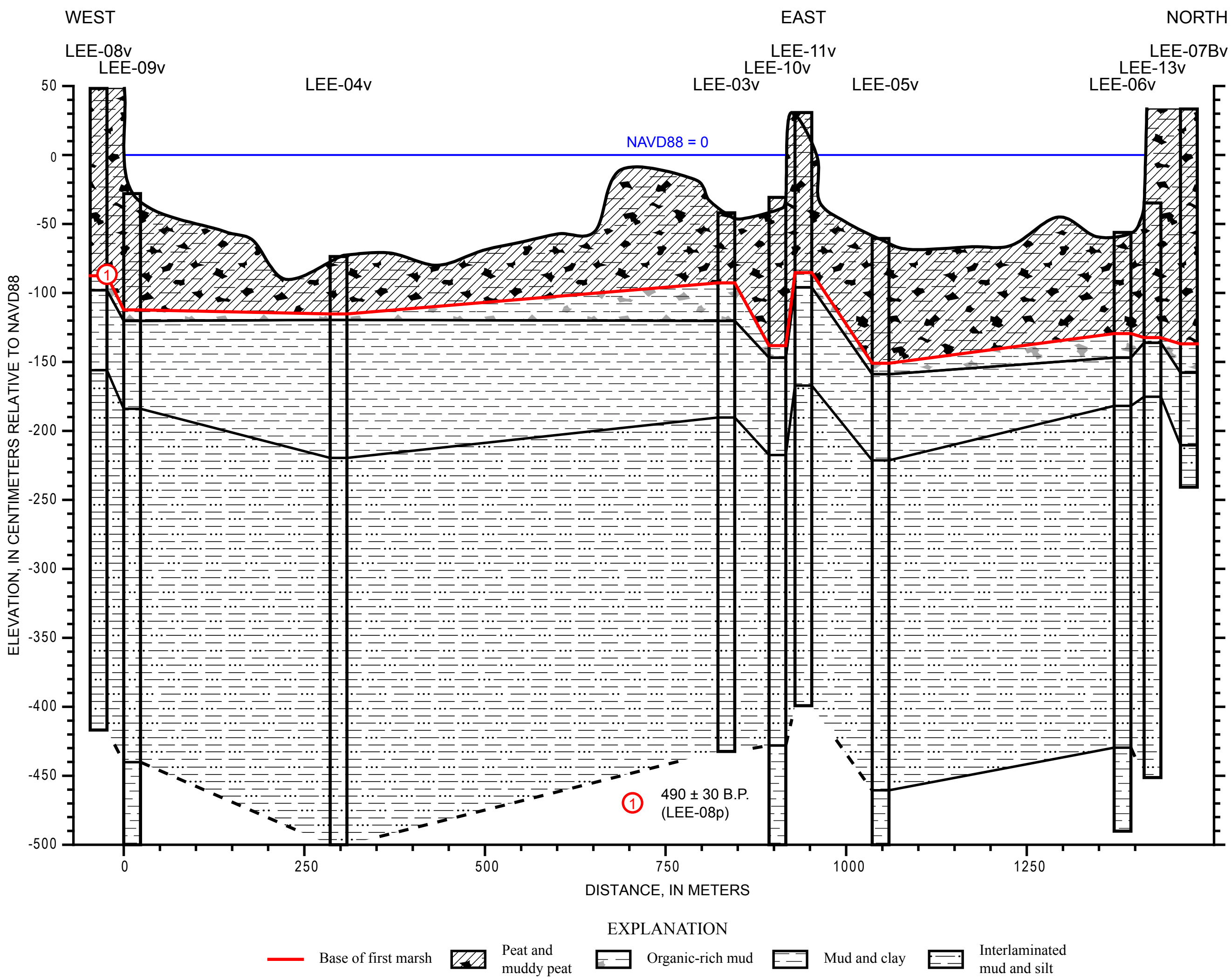

Figure 12. Combined bathymetric profile and stratigraphic cross section for marsh and open-water cores LEE-08v to LEE-07Bv illustrating the magnitude of subsidence and wetland erosion (in centimeters) at the Leeville study area. Highlighted contact is the base of the facies 1 first marsh (in red); associated radiocarbon age is from table 2. Core locations are shown in figure 11; vertical scale is greatly exaggerated.

FCN-09v). The linear decompaction method was used to adjust sediment-contact depths and elevations for the purpose of estimating magnitudes of subsidence and erosion (table 1).

The generalized stratigraphic succession at Fourchon consists of five or six sedimentary facies depending on location with respect to the delta-plain setting. From youngest to oldest, the facies are: (1) muddy peat with roots, (2) peat, (3) organic-rich mud, (4) mostly massive mud, (5) interbedded mud and muddy sand, and (6) oyster shells in a muddy matrix. Facies 1 is restricted to core sites FCN-01 and FCN-02 (fig. 14) and either was not deposited or was removed by erosion from the adjacent open-water coring sites. This facies, which overlies poorly developed peat, represents recent mud deposition and marsh aggradation possibly associated with disposal of sediment dredged from nearby canals. Another possible sediment source for recently deposited mud would be the regional shoreline retreat and associated transgression of the delta plain along the Caminada-Moreau headland (Ritchie and Penland, 1985). However, the redistribution of eroded mud deposited in the adjacent marshes during storm flooding would be expected at all the coring sites, not just those to the west.

The facies 2 peat, which represents the first widespread marsh development, is thin and poorly developed at core sites FCN-01 and FCN-02. Where the peat section is relatively thick, it contains interspersed and interbedded mud. The facies 3 organic-rich mud is well developed at core sites FCN-01, FCN-02, and FCN-03 but is thin to absent east of core FCN-04v (fig. 14). Finely broken shell fragments occur throughout facies 5, indicating moderately high energy and particle transport. The dense concentration of articulated oyster valves and large fragments that compose facies 6 is indicative of in-situ conditions of an oyster reef.

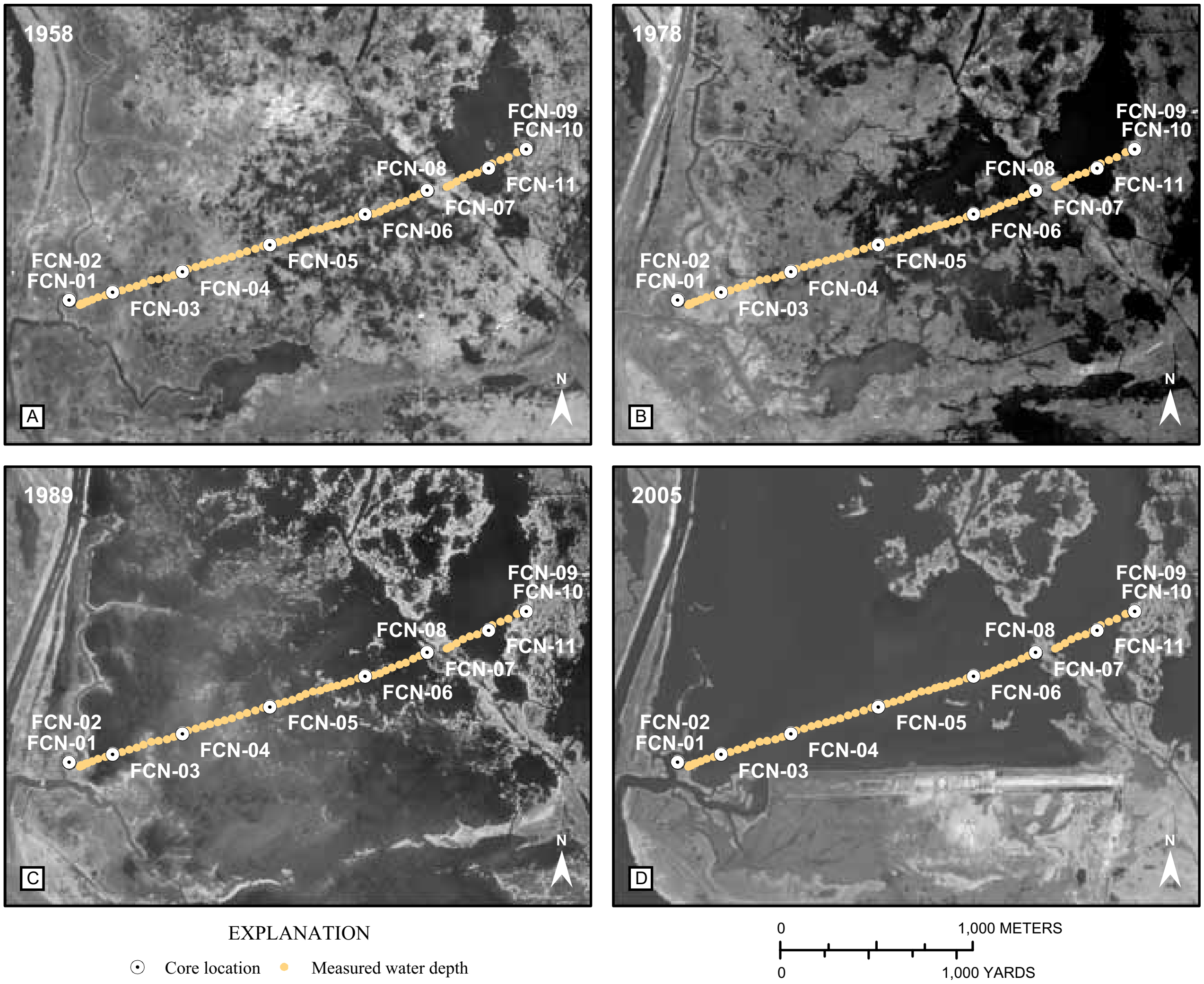

Figure 13. Locations of sediment cores and sediment-surface profiles from the Fourchon study area superimposed on aerial photographs taken in (A) 1958, (B) 1978, (C) 1989, and (D) 2005. Image sources are (A) Edgar Tobin Aerial Surveys controlled aerial mosaic for Leeville quadrangle, source imagery acquired October 1958; (B) U.S. Geological Survey (USGS) black-and-white aerial photography acquired March 27, 1978; (C) and (D) USGS Digital Orthophoto Quarter Quadrangles (DOQQ) for southwest quadrant of Leeville quadrangle, source imagery acquired November 18, 2005.

At Fourchon, accommodation space associated with land-water changes ranged from 39 cm (FCN-02v) to 111 cm (FCN-03v) and averaged about 85 cm. In general, the physical setting controlled which process was responsible for creating the accommodation space. Subsidence was greater than erosion at most of the open-water coring sites, whereas erosion was greater than subsidence at most of the marsh-edge coring sites. Marsh-sediment erosion ranged from 22 to 72 cm and averaged about 40 cm, whereas subsidence ranged from 14 to 78 cm and averaged about 45 cm (table 1). The maximum subsidence estimate, which was at FCN-04v, may be slightly exaggerated as a result of the compaction adjustment.

Caminada

The Caminada study area also occupies a lower delta-plain setting of the Lafourche subdelta, but it is distinctly different from the others because it is located landward of the prominent Caminada-Moreau beach-ridge complex (fig. 4). The beach ridges were constructed by waves reworking sediment at the mouth of Bayou Moreau when it was an active distributary channel flowing into the Gulf of Mexico. The beach-ridge elevations are high enough to protect the Caminada study area from waves during extreme storm-overwash events. Comparison of wetland distribution on aerial photographs between 1958 and 1978 shows that marshes were nearly

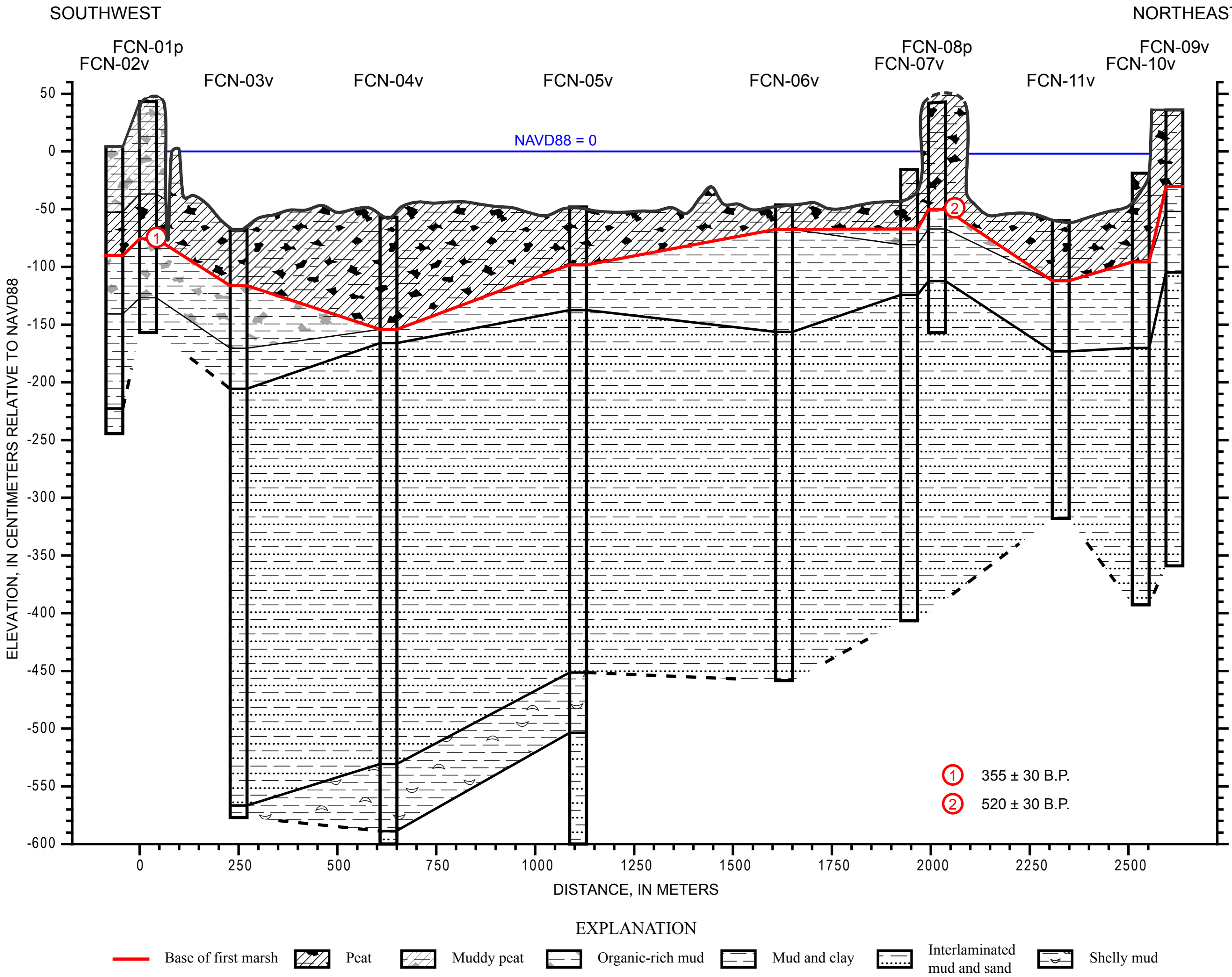

Figure 14. Combined bathymetric profile and stratigraphic cross section for marsh and open-water cores FCN-02v to FCN-09v illustrating the magnitude of subsidence and wetland erosion (in centimeters) at the Fourchon study area. Highlighted contact is the base of the facies 2 first marsh (in red); associated radiocarbon ages are from table 2. Core locations are shown in figure 13; vertical scale is greatly exaggerated.

continuous where the cores were collected, and the conversion of land to water occurred primarily after 1978 (fig. 15). By 1998 (not shown in fig. 15) there was more water than land, and by 2004 almost all of the formerly emergent marsh between the core sites and the beach-ridge complex to the south was open water. The Caminada area was selected for investigation because of its proximal beach-ridge setting and the late timing of rapid interior wetland loss.

Marsh elevations at Caminada range from 21 to 40 cm (figs. 16 and 17). Water depths, which range from only a few centimeters to -66 cm and average about -40 cm, are relatively shallow and consistent across the area that was formerly emergent marsh. Core shortening was significant at Caminada with 13 of the 17 vibracores undergoing more than 20 percent shortening. The other four vibracores underwent minor shortening. To estimate erosion and subsidence at Caminada, the decompacted depths of the basal-organic contact in marsh-edge or open-water vibracores were obtained using the linear adjustment method.

The shallow stratigraphy at Caminada consists of five sedimentary facies: (1) peat, (2) organic-rich mud, (3) massive mud, (4) oyster shells in a muddy matrix, and (5) interlaminated mud. Organic material makes up a high percentage of the facies 1 peat for most of the cores, although two cores (CAM-01v and CAM-02v) encountered some interbedded mud near the basal contact. In the push cores (CAM-09p,

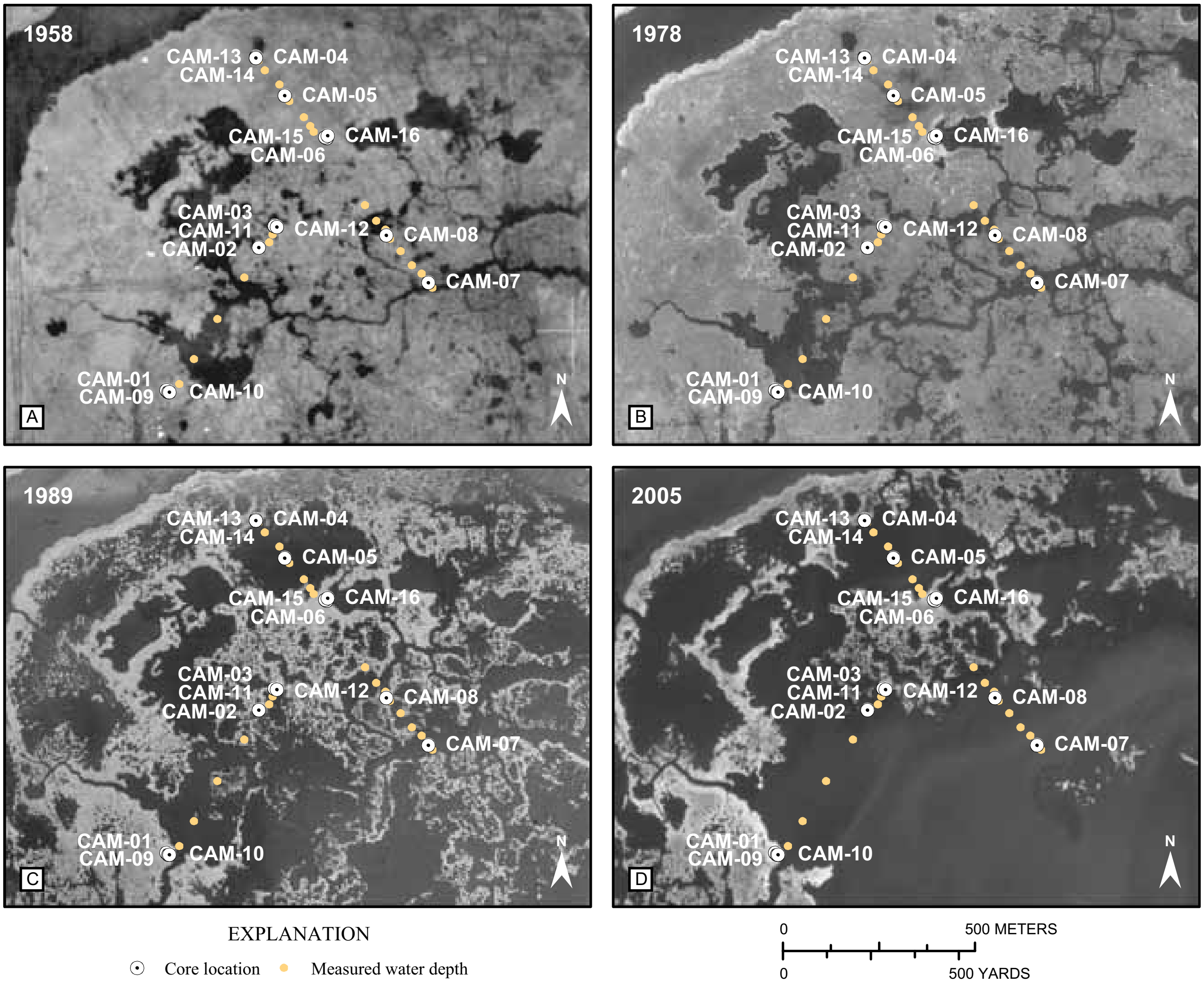

Figure 15. Locations of sediment cores and sediment-surface profiles from the Caminada study area superimposed on pre- and post-subsidence aerial photographs taken in (A) 1958, (B) 1978, (C) 1989, and (D) 2005. Image sources are (A) Edgar Tobin Aerial Surveys controlled aerial mosaic for Leeville quadrangle, source imagery acquired October 1958; (B) U.S. Geological Survey (USGS) black-and-white aerial photography acquired March 27, 1978; (C) and (D) USGS Digital Orthophoto Quarter Quadrangles (DOQQ) for northeast and southeast quadrants of Leeville quadrangle, source imagery acquired November 18, 2005.

CAM-11p, CAM-13p, and CAM-15p) facies 1, which represents the first widespread marsh development, is between 120 and 150 cm thick. The facies 2 organic-rich mud is thicker in the western part of the study area and is thinner or absent along the eastern transect. Facies 4, an oyster bed, was only encountered in the north-central part of the study area between marsh-core sites CAM-04 and CAM-16. Facies 5, interlaminated mud, is identified by its color and textural bands that are apparent because the layers contain more silt or sand. In a few cores, the muddy sediments contain rare fragments of shell.

Marsh push cores CAM-09p, CAM-11p, CAM-13p, and CAM-15p recovered organic-sediment sections that are thicker than the equivalent decompacted peat thicknesses in vibracores from the same sites. The peat-mud contact in push core CAM-13p (150 cm) is deeper than in any other push core by more than 20 cm, and it is generally deeper than the linear-adjusted depths for the same contact in all the marsh-edge and open-water vibracores. Consequently, CAM-13p cannot be used to estimate erosion and subsidence. Core CAM-15p is common to both cross sections (figs. 16 and 17). It is a substitute for CAM-06v, which underwent the most compaction. At Caminada, accommodation space associated with land-water changes ranged from 47 cm (CAM-16v) to 104 cm (CAM-07v) and averaged about 75 cm. The accommodation space was created mostly by erosion, which was substantially greater than subsidence at most of the coring sites where measurements could be made. Marsh-sediment erosion ranged from 44 to 81 cm and averaged about 60 cm, whereas subsidence ranged from 2 to 38 cm and averaged about 15 cm (table 1).

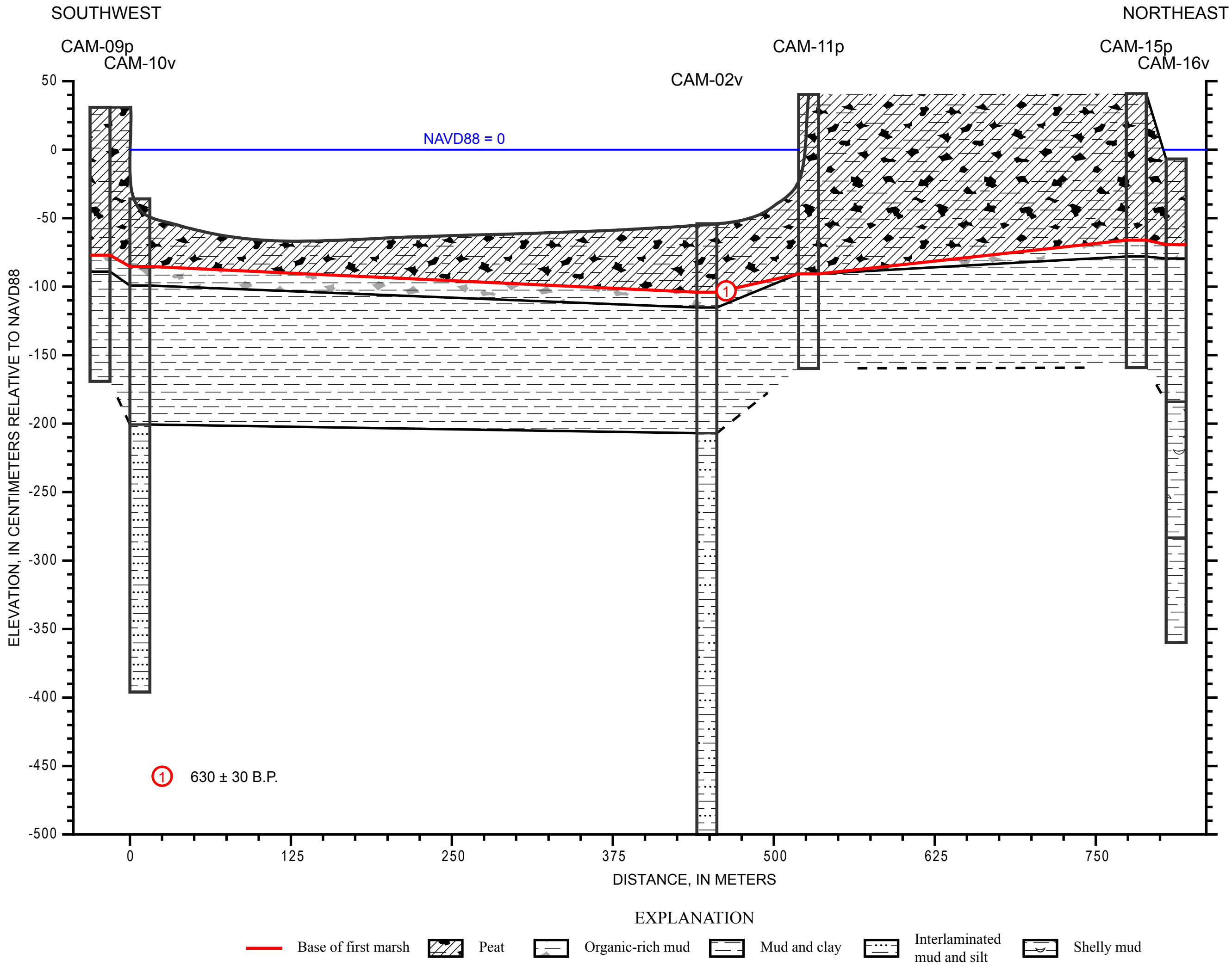

Figure 16. Combined bathymetric profile and stratigraphic cross section for marsh and open-water cores CAM-09p to CAM-16v illustrating the magnitude of subsidence and wetland erosion (in centimeters) at the Caminada study area. Highlighted contact is the base of the facies 1 first marsh (in red); associated radiocarbon age is from table 2. Core locations are shown in figure 15; vertical scale is greatly exaggerated.

Subsurface-Fluid Production Near Coring Sites

Oil, gas, and associated formation water have been produced for decades in coastal Louisiana, and some of the historical land-water conversion can be attributed to direct removal of wetlands associated with dredging of access canals for drilling rigs (Day and others, 2000). The producing fields that may have influenced observed land-water changes in Barataria basin are discussed in this section. Annual volumes of produced oil and gas are available for individual fields since production began. However, annual volumes of produced formation water are available only since 1965. Therefore, water volumes produced at a field before 1965 are not included in the history of fluid production.

The Bayou Perot coring site is essentially surrounded by the Barataria and Bayou Perot fields to the north, the Delta Farms fields to the northwest, the Lafitte field to the east, and the Little Temple and Little Lake fields to the south (fig. 2). The Ironton coring site is northeast of the large Lafitte field, and the Leeville coring site is on the southeastern flank of the large Leeville field. The Fourchon and Caminada sites are located between the Leeville field and the north flank of the giant Bay Marchand field, which is located mostly offshore, but produces beneath the land near Fourchon.

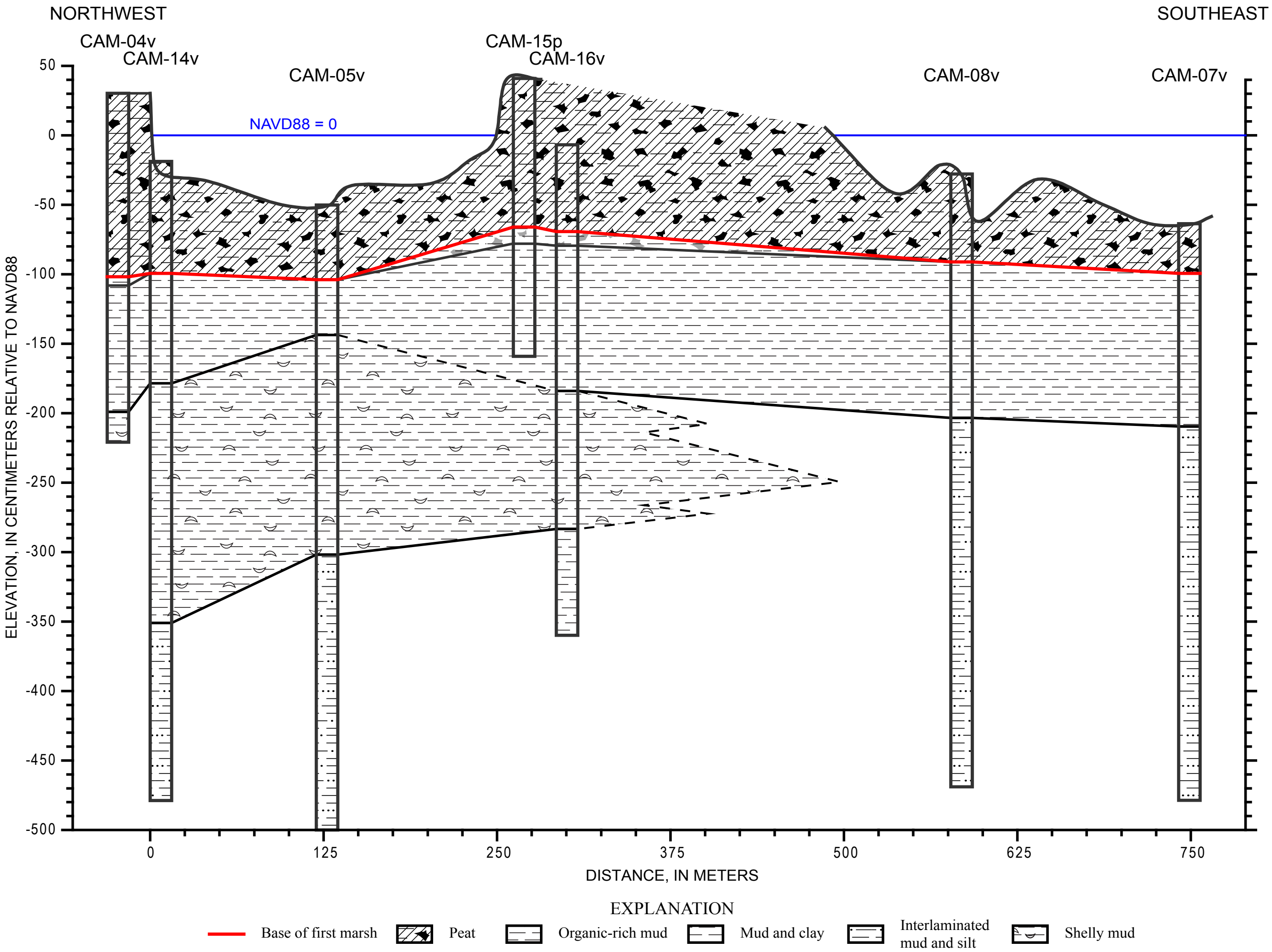

Figure 17. Combined bathymetric profile and stratigraphic cross section for marsh and open-water cores CAM-04v to CAM-07v illustrating the magnitude of subsidence and wetland erosion (in centimeters) at the Caminada study area. Highlighted contact is the base of the facies 1 first marsh (in red). Core locations are shown in figure 15; vertical scale is greatly exaggerated.

Barataria and Bayou Perot Fields

The Barataria-Bayou Perot field complex consists of four structurally separated hydrocarbon accumulations identified individually as the Barataria, Barataria West, Barataria South, and Bayou Perot fields (fig. 3). For purposes of discussing regional subsurface-fluid withdrawal, the reported volumes of produced fluids are combined as a single field because of their close proximity. The Barataria-Bayou Perot complex produces from about 25 middle to late Miocene sand reservoirs. The reservoirs are structurally controlled by faults over a deep-seated salt dome that forms a low-relief domal closure (Wallace, 1944; Hamilton, 1983). From 1939, when they were discovered, through 2005, this collection of fields has produced more than 55 million barrels (bbls) of oil, 166 billion cubic feet (Bcf) of gas, and 115 million bbls of water from more than 150 wells. Oil production peaked in the late 1940s and early 1950s, whereas water and gas production peaked in the mid- to late 1960s and late 1960s to early 1970s, respectively (fig. 18). Oil production from Barataria field and gas production from Barataria South field accounted for more than half the total combined production from the field complex.

Delta Farms Fields

For purposes of regional volumetric analysis, hydrocarbon production for the Delta Farms and West Delta Farms fields were combined, even though the fields are separated structurally. The primary field was discovered in 1940, whereas the western extension was discovered in 1952. The field, which overlies a deep-seated salt dome, is bisected by an east-west growth fault that is downthrown to the south (Morgan, 1953). Through 2005, the fields produced more than 133 million bbls of oil, 346 Bcf of gas, and 342 million bbls of water. Production was from as many as 35 middle to late Miocene sand reserviors (Bausfield, 1983a; 1983b) that were penetrated by more than 250 wells. Most of the productive wells of the Delta Farms field directly underlie Bayou Perot and the marshes immediately west of Bayou Perot. Oil-and-gas production accelerated from the mid-1940s to the early and late 1950s (oil and gas, respectively), when they peaked and then went into decline (fig. 19). Maximum water production, which lagged behind the other fluids, peaked about 1965.

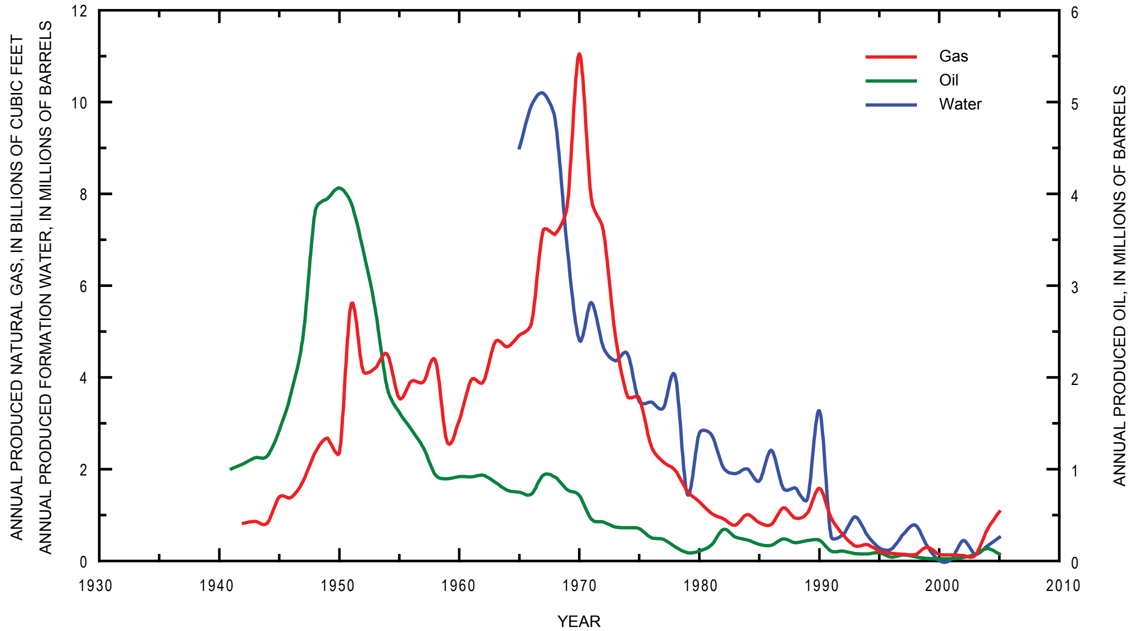

Figure 18. Annual fluid production through 2005 from the Barataria, Barataria South, Barataria West, and Bayou Perot fields in Lafourche Parish. Data from Louisiana Department of Natural Resources (LDNR) and PI/Dwights PLUS database (IHS Inc., 2007).

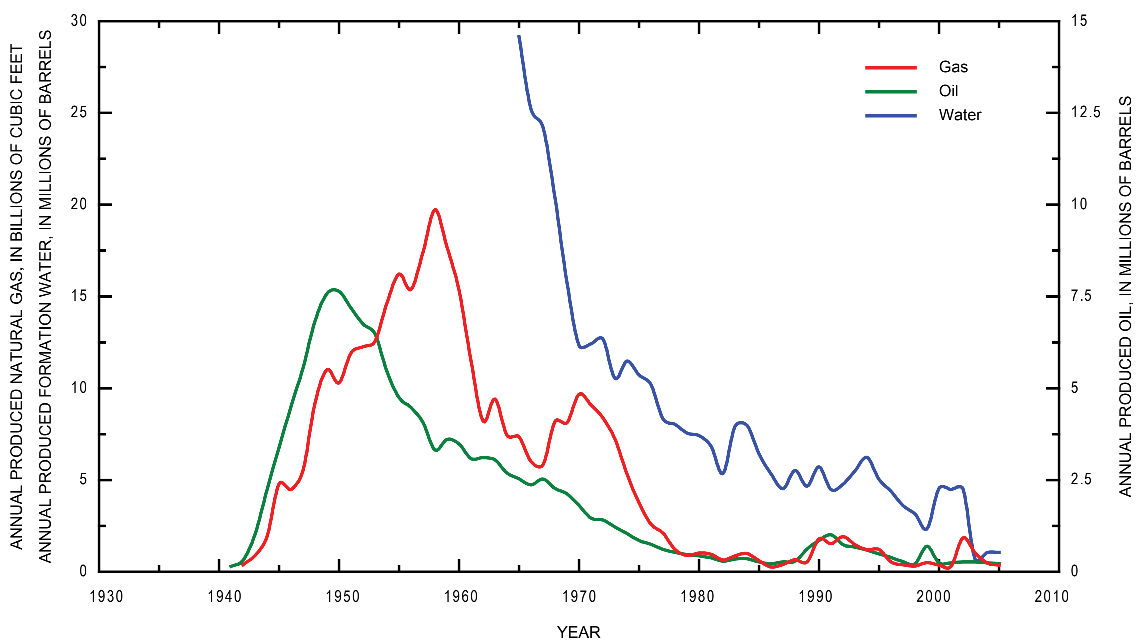

Figure 19. Annual fluid production through 2005 from the Delta Farms and Delta Farms West fields in Lafourche Parish. Data from Louisiana Department of Natural Resources (LDNR) and PI/Dwights PLUS database (IHS Inc., 2007).

Little Temple and Little Lake Fields

Hydrocarbon accumulation in the Little Lake field and adjacent Little Temple field is structurally trapped by three down-to-the-south faults that cross a southerly plunging anticline (Swords, 1965). The fields have produced from about 15 middle to upper Miocene sand reservoirs at depth ranging from 2,600 to 4,000 m. From their discovery in 1948 through 2005, the fields have produced more than 64 million bbls of oil, 156 Bcf of gas, and 142 million bbls of water from more than 200 wells. Oil-and-gas production from Little Lake field, which accounted for more than 80 percent of the combined production for these fields, was sustained at moderate rates between 1955 and 1970, whereas maximum water production lagged behind the other fluids by about 5 years (fig. 20). Oil-and-gas production from the Little Temple field began to accelerate from about 1955 to 1960, but then declined slowly before accelerating rapidly and peaking about 1970. Water production also peaked about 1970. Since 1980, fluid withdrawal from the Little Temple field has been primarily gas and water (fig. 20).

Lafitte Field

The Lafitte field, which also overlies a deep-seated salt dome (Wallace, 1944), has been a prolific producer since it was discovered in 1935. The productive sand reservoirs, which range from middle Miocene to Pliocene, occur at depths from greater than 3,900 m to less than 1,000 m. A three-dimensional seismic survey in 1990 guided an infill drilling program (1992-1996) that targeted oil production from Pliocene channel sands less than 1,200 m deep (Greene, 1998). By 2005, the field had yielded more than 260 million bbls of oil, 310 Bcf of gas, and 699 million bbls of water from approximately 700 wells that penetrated 50 reservoirs (Greene, 1998). Most of the production accelerated in the middle to late 1960s, peaked about 1970 and then went into rapid decline except for water production, which declined more slowly as the life of the field was prolonged. A minor secondary resurgence in gas production occurred about 2000 (fig. 21). The largest tracts of wetland loss above and adjacent to the Lafitte field, which developed between 1956 and 1990, are located north of the salt dome, extending in a more than 2-km wide swath from Barataria Waterway east to the Mississippi River levee system (fig. 3). Land losses directly over the Lafitte field salt dome are more localized and are generally restricted to areas where marsh sediments were dredged for access canals.

Leeville Field

The Leeville field, which overlies a piercement salt dome, was discovered in 1928 and has been producing subsurface fluids from upper Miocene and Plio-Pleistocene growth-faulted strata since 1931 (Anonymous, 1983). Through 2005, the field had produced more than 128 million bbls of oil, 282 Bcf of gas, and 163 million bbls of water from more than 650 wells. Oil-and-gas production peaked and stabilized from the middle 1950s to the early to late 1970s (oil and gas, respectively), with a second spike in gas production in the early 2000s. Water production also peaked in the early 1970s (fig. 22). Most of the producing wells are located over the Leeville salt dome, which is centered west of Bayou Lafourche, about 3.5 km northwest of the core sites (fig. 3). However, the closest production wells are less than 1,000 m west of core site LEE-01v. The largest tracts of wetland loss, which developed between 1978 and 1990, are on the east and southeast flanks of the Leeville field where shallow (<1,000 m) basal-Pleistocene strata produce gas (Sabate, 1968). Directly above the Leeville field salt dome, land losses primarily occurred prior to 1978 and are restricted mostly to the dredged access canals.

Geological Rates of Subsidence and Aggradation

Rates of vertical sediment accumulation between delta-plain peats have been used as a proxy for long-term, time-averaged subsidence rates (Penland and others, 1988; Roberts and others, 1994; Kulp and Howell, 1998). These calculations assume that the accommodation space necessary for vertical sediment accumulation (aggradation) was provided by subsidence regardless of the specific process (crustal loading, sediment compaction, fault activation). This assumption seems to be valid as a first approximation for wetland sediments in deltaic settings and static sea-level conditions. The condition of uniform sea level essentially equivalent to modern sea level is not difficult to achieve for decades or a few centuries, but would not be a reasonable assumption for periods encompassing several millennia. To avoid possible complications associated with eustatic fluctuations, only subsidence rates for periods less than 2,500 yr were included in the comparison.

Geological rates of subsidence calculated using the depth method range from 1.1 to 4.1 mm/yr (table 2) and average about 1.9 mm/yr. Subsidence rates calculated from the interval method are similar, ranging from 0.3 to 6.7 mm/yr (table 2) and averaging about 1.4 mm/yr. The maximum depth-method subsidence-aggradation rate calculated from radiocarbon data for Bayou Perot (2.6 mm/yr) compares favorably with 3 mm/yr reported for the same area by Kosters and others (1987).

Historical Land-Surface Subsidence Measurements

Rates of land-surface subsidence have traditionally been calculated as the reductions in land elevations during a specific period. The subsidence epoch may range in length from years or decades (historical time scale) to centuries or millennia

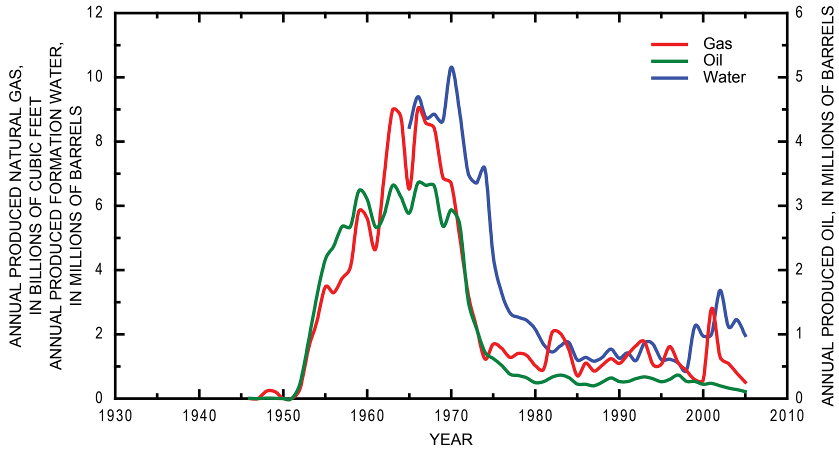

Figure 20. Annual fluid production through 2005 from the Little Temple and Little Lake fields in Lafourche Parish. Data from Louisiana Department of Natural Resources (LDNR) and PI/Dwights PLUS database (IHS Inc., 2007).

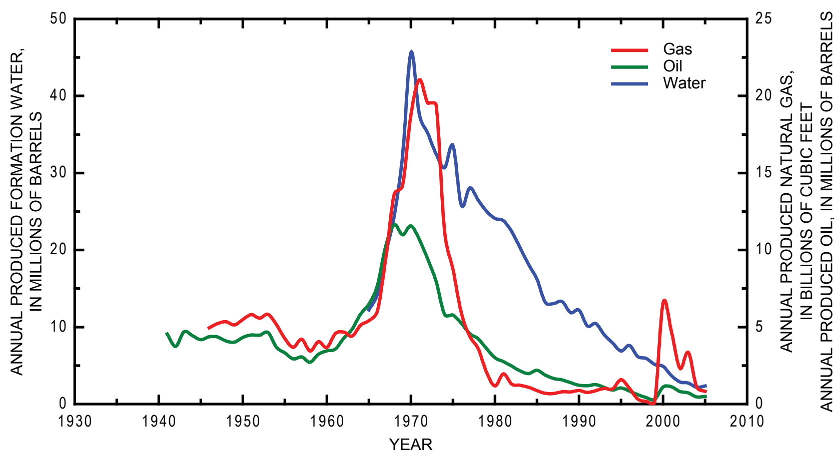

Figure 21. Annual fluid production through 2005 from the Lafitte field in Jefferson Parish. Data from Louisiana Department of Natural Resources (LDNR) and PI/Dwights PLUS database (IHS Inc., 2007).

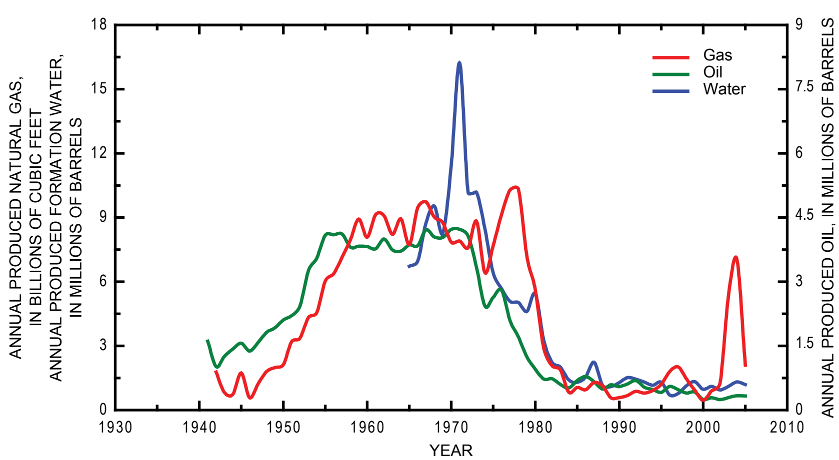

Figure 22. Annual fluid production through 2005 from the Leeville field in Lafourche Parish. Data from Louisiana Department of Natural Resources (LDNR) and PI/Dwights PLUS database (IHS Inc., 2007).

(geological time scale). The resulting time-averaged rates of subsidence at both time scales are not constant and can vary both temporally and spatially. For purposes of coastal-resources management, coastal-restoration planning, and subsidence prediction, the most critical data are the most recent rates of subsidence (past 5 to 10 yr). The most reliable estimated rates of subsidence are determined from elevation changes measured by precision instruments at land-based stations that are referenced to one another within a regional network.

The National Geodetic Survey (NGS), a branch of the National Oceanic and Atmospheric Administration (*http://www.ngs.noaa.gov*), is the Federal agency responsible for maintaining a countrywide network of geodetic control stations used to establish geographic positions and elevations. The geodetic network consists of benchmarks and GPS-based Continuously Operating Reference Stations (CORS).

Tide-Gage Records

Tide gages primarily record short-term fluctuations in water level, but they also can be used to document vertical land motion if the records are of good quality and long enough (~60 yr) that trends can be established (Douglas, 2001). Tide-gage records are noisy because they include interannual and decadal secular variations that are related to meteorological and climatic forcing, and they include the global rise in sea level of about 1.8 mm/yr during the past century (Douglas, 2001).

The Leeville, Fourchon, and Caminada coring sites are close enough to the tide gage at Grand Isle that its record can be used as a proxy for general subsidence rates (Shinkle and Dokka, 2004). Water levels have been recorded at Grand Isle nearly continuously since 1947 (fig. 23). Annual mean sea-level data, representing average water levels for an entire year, show an overall relative sea-level rise (RSLR) related to subsidence, but the rates of sea-level rise for different periods are not constant (fig. 23). When the tide-gage record is divided into periods matching the NGS leveling epochs of 1965 and 1993, it shows that rates of RSLR accelerated from about 3.3 mm/yr between 1947 and 1965 to about 10.7 mm/yr between 1965 and 1993. Since 1993, rates of RSLR have declined to about 4.1 mm/yr (fig. 23). Dividing the record based on inflections in the data instead of benchmark-survey epochs shows that the rates of RSLR accelerated from about 2.2 mm/yr between 1947 and 1964 to about 11.5 mm/yr between 1964 and 1991 and then declined to about 3.4 mm/yr since 1991. All of these rates of RSLR are unadjusted for the eustatic component, which would make inferred subsidence rates slightly lower.

Statistical covariance analysis of the tide-gage data was conducted to determine if the rates of RSLR (slopes of linear regression) for each of the three periods were significantly different. The tests of significance demonstrate that rates of RSLR for 1947 to 1964/65 and 1991/93 to 2006 were both significantly lower ($p < 0.01$) than the higher RSLR rate for 1964/65 to 1991/93.

The NOS tide gage closest to Grand Isle that is in a relatively stable geological setting is at Pensacola, FL (Holdahl and Morrison, 1974). Historical records at Pensacola from 1924 to 2006 show a relatively uniform rate of RSLR of 2.1 mm/yr (fig. 23). Periods of pronounced RSLR acceleration and deceleration comparable to those at Grand Isle are not present in the Pensacola data. The absence of short-term periods of increased and decreased rates of relative sea-level rise at Pensacola indicate that processes responsible for those changes at Grand Isle, such as subsidence, either are not operating at Pensacola or are operating at rates that cannot be detected in the data.

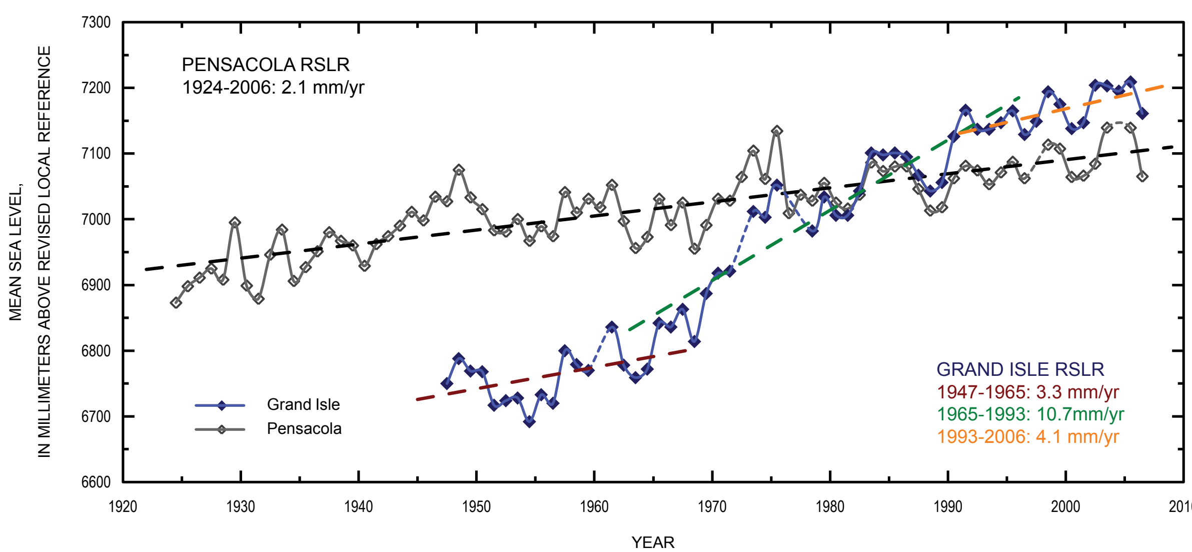

Figure 23. Linear-regression trends for mean annual water levels recorded at the Grand Isle, LA tide gage between 1947 and 2006 and at the Pensacola, FL tide gage between 1924 and 2006. Data from the Permanent Service for Mean Sea Level website (PSMSL; http://www.pol.ac.uk/psmsl/). For Grand Isle, the Revised Local Reference (RLR) is 5,214 mm below the station datum; for Pensacola, RLR is 4,312 mm. RSLR, relative sea-level rise.

Benchmark Surveys

In southeastern Louisiana, surveyors established three lines of benchmarks along roads that follow the natural levees of major distributaries of the Mississippi delta. The eastern line parallels the modern Mississippi River (figs. 1 and 24) and extends from Chalmette to Venice (State highway LA 23), a central line runs along Bayou Lafourche (figs. 1 and 25) from Raceland to Grand Isle (State highway LA 1), and the western line follows Bayou Petit Calliou from Houma to Cocodrie (State highway LA 56). The leveling lines are oriented roughly north and south across the regional structural grain, and they encompass a large area where historical rates of wetland loss were high (Morton and others, 2006; Barras and others, 2008).

The lines of benchmarks are referred to as leveling lines because leveling was the surveying technique originally used to determine benchmark positions and elevations. Benchmark elevations relative to a starting benchmark were surveyed along the leveling lines in 1938, 1951, 1964, and 1971 (Mississippi River line); 1952 or 1955, 1965, 1982, and 1993 (Bayou Lafourche line); and 1966 and 1993 (Bayou Petit Caillou line). Although very few benchmarks are present on all the surveys, general trends can be identified by comparing magnitudes and average rates of subsidence for the same area and for consecutive periods (fig. 26; tables 4 and 5). NGS provided subsidence rates for the 1952/55 to 1965 epoch along Bayou Lafourche; subsidence rates for the 1965-1982 and 1982-1993 epochs along Bayou Lafourche as well as all subsidence rates along the Mississippi River and Bayou Petit Caillou were calculated by Shinkle and Dokka (2004). Subsidence rates based on benchmark surveys since 1993 have not been reported. In 2003, the benchmarks from Raceland to Grand Isle (Bayou Lafourche) and from Belle Chase to Venice (Mississippi River) were reoccupied using a combination of static (stationary) and kinematic (moving) GPS surveys. However, those surveys were conducted for evaluating hurricane evacuation routes rather than generating historical rates of subsidence.

The Ironton coring sites are about 7.5 km from the closest reoccupied benchmarks along State highway LA 23 (fig. 24), which was built on the artificially raised levee of the Mississippi River. Average subsidence rates along the Mississippi River (fig. 26) north of the Lake Washington-Empire Fault area first increased from about -17 mm/yr between 1938 and 1951 to about -20.1 mm/yr between 1951 and 1964 and then systematically decreased to about -10 mm/yr from 1971 to 1984. Comparable rates are obtained from those benchmarks closest to the Ironton coring sites (table 4). There subsidence rates first increased from about -14 mm/yr between 1938 and 1951 to about -20.3 mm/yr between 1951 and 1964 and then systematically decreased to about -10.7 mm/yr from 1971 to 1984. The temporal increases in wetland loss at Ironton do not correlate with the temporal decreases in subsidence rates at the nearest benchmarks. Average subsidence rates at benchmarks south of Lake Washington were substantially higher than to the north, but also decreased from greater than -25 mm/yr between 1964 and 1971 to about -18 mm/yr between 1971 and 1984.

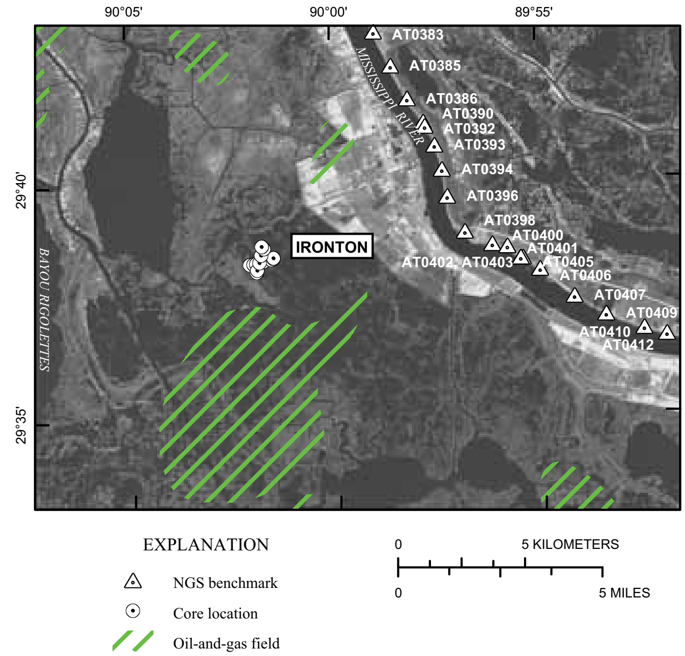

Figure 24. Locations of resurveyed benchmarks nearest the Ironton study area. Landsat 5 Thematic Mapper (TM) image acquired October 28, 2006; visual display uses band 4 (near-infrared). NGS, National Geodetic Survey.

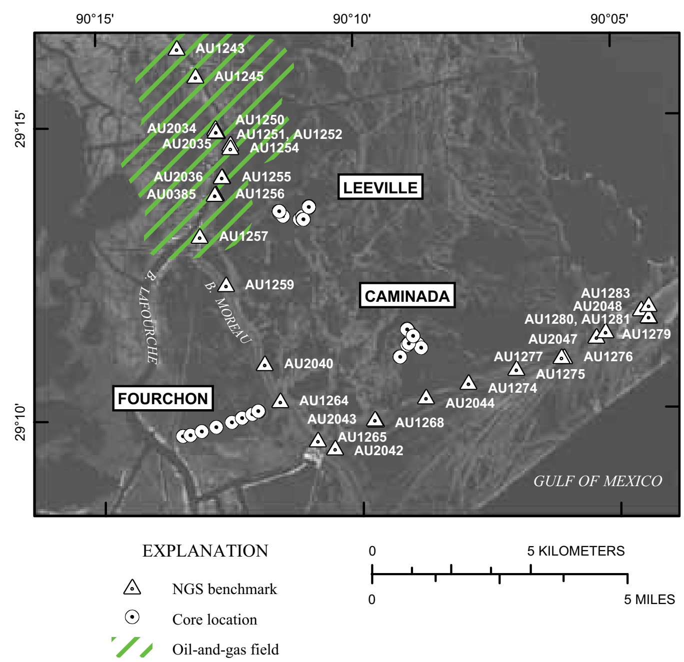

Figure 25. Locations of resurveyed benchmarks nearest the Leeville, Fourchon, and Caminada study areas. Landsat 5 Thematic Mapper (TM) image acquired October 28, 2006; visual display uses band 4 (near-infrared). NGS, National Geodetic Survey.

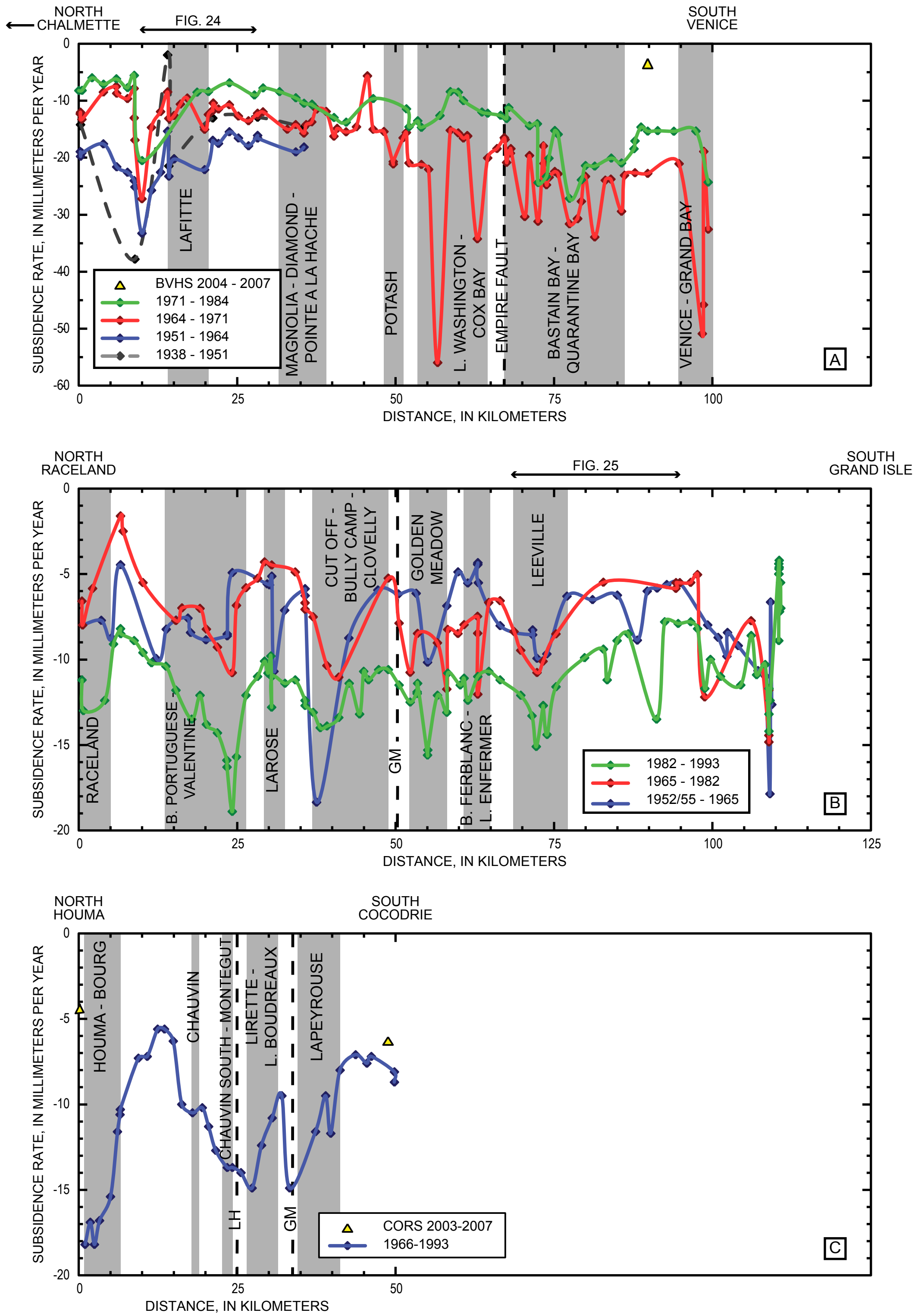

Figure 26. Historical subsidence rates calculated by the National Geodetic Survey from repeat leveling surveys at benchmarks along (A) State highway LA 23 between Chalmette and Venice, (B) State highway LA 1 between Raceland and Grand Isle, and (C) State highway LA 56 between Houma and Cocodrie. Benchmark locations shown in figures 24 and 25 are indicated on plots (A) and (B), respectively. Recent subsidence rates derived from GPS measurements are plotted as filled triangles in (A) and (C). Shaded areas delineate approximate productive boundaries of nearby oil-and-gas fields; dashed vertical lines show projected intersection with subsurface faults. Profile distances increase from north to south. GM, Golden Meadow fault; LH, Lake Hatch spur fault.

Table 4. Historical subsidence rates at benchmarks along the Mississippi River east of the Ironton study area.

[Data from the National Geodetic Survey (Shinkle and Dokka, 2004). Geographic locations of these benchmarks are illustrated in figure 24. Abbreviations: PID, Permanent Identifier; mm/yr, millimeters per year]

PID	Station Name	1938-1951 (mm/yr)	1951-1964 (mm/yr)	1964-1971 (mm/yr)	1971-1984 (mm/yr)
AT0383	U 151 USE		-33.28	-27.25	-20.53
AT0385	V 151 USE		-25.74	-14.72	
AT0386	W 151 USE		-22.56	-11.95	
AT0390	28 BOLT	-1.98	-15.37	-8.50	
AT0392	3168 LAGS	-21.47	-23.28	-13.14	
AT0393	3170 LAGS	-20.21	-20.27	-12.64	
AT0394	M 194			-10.64	
AT0396	N 194			-9.58	
AT0398	D 281				-8.53
AT0400	Y 151 USE		-22.13	-15.07	
AT0401	P 194			-12.45	-8.42
AT0403	27 BOLT	-13.06	-17.01	-11.67	
AT0402	27 CAP		-16.99	-11.80	
AT0405	PL 11 USGS			-10.45	
AT0406	Z 151		-17.54	-11.51	
AT0407	A 152		-15.49	-10.75	-6.88
AT0409	B 152 USE		-16.58	-12.74	
AT0410	C 152 USE		-17.95	-13.57	
AT0412	E 281				-9.02
Mean		**-14.18**	**-20.32**	**-12.85**	**-10.68**

The Leeville, Fourchon, and Caminada coring sites are reasonably close (1 to 2.5 km) to reoccupied benchmarks along State highway LA 1 (fig. 25). Re-leveled benchmark data along LA 1 (fig. 26B) show that average subsidence rates for each epoch between 1952/55 and 1982 increased slightly from -7.8 mm/yr to -7.9 mm/yr and then accelerated to -11.1 mm/yr between 1982 and 1993. Nearly identical results are obtained from those benchmarks closest to the coring sites (table 5). At those benchmarks, average subsidence rates for each epoch between 1952 and 1982 increased slightly from -7.3 mm/yr to -7.7 mm/yr and then accelerated to -11.3 mm/yr between 1982 and 1993. The general trend of wetland loss at the Leeville, Fourchon, and Caminada coring sites after 1978 generally agree with the increased subsidence rates for the same period.

Four benchmarks near coring sites along State highway LA 1 were surveyed sequentially between 1965 and 1993 (table 5). The average subsidence rate of -9.6 mm/yr calculated for the four benchmarks is remarkably similar to the -10.7 mm/yr rate inferred from data recorded over the same period at the nearby Grand Isle tide gage (fig. 23). Although the benchmark-elevation data are useful for establishing historical trends, the lack of data after 1993 prevents using this time series to determine the most recent subsidence rates.

Continuously Operating Reference Stations

Continuously Operating Reference Stations (CORS) utilize building-mounted GPS receivers to monitor land-elevation changes continuously with high precision. Three CORS installations operating in southeastern Louisiana (HOUM, LMCN, and BVHS) encompass the field-study sites (fig. 1). Because the GPS solutions are for a single point, the low spatial density of stations leaves large gaps in the regional coverage, and CORS locations within the geologic setting may not be optimal for characterizing regional subsidence rates and patterns. Still, recent elevation changes detected at the three GPS stations likely have important implications regarding rates of subsidence and regional wetland loss in southeastern Louisiana. At the very least, they provide the most recent accurate measurement of vertical motion in the Mississippi delta plain.

The CORS in southeastern Louisiana are recent additions to the North American network of geodetic control. Stations were established at Boothville (BVHS) in 2002 and at Houma (HOUM) and Cocodrie (LMCN) in 2003. Because GPS signals are influenced by many variables, including atmospheric conditions, the signal-to-noise ratio in the data is low, and

Table 5. Historical subsidence rates at benchmarks along State highway LA 1 that are near the Leeville, Fourchon, and Caminada coring sites.

[Data from the National Geodetic Survey. Geographic locations of these benchmarks are illustrated in figure 25. Abbreviations: PID, Permanent Identifier; mm/yr, millimeters per year]

PID	Station Name	1952-1965 (mm/yr)[1]	1965-1982 (mm/yr)[2]	1982-1993 (mm/yr)[2]	1965-1993 (mm/yr)[1]
AU1243	D 221		-8.37		
AU1245	E 221		-9.47	-12.10	-10.52
AU2034	P 359			-13.30	
AU1250	LEEVILLE	-8.03			
AU1251	LEEVILLE RM 2	-8.56			
AU1252	LEEVILLE RM 1	-8.28			
AU2035	N 359			-15.10	
AU1254	P 154	-9.94	-10.77		
AU2036	JESSE RM 1			-12.70	
AU1255	JESSE		-10.11	-12.70	-11.14
AU0385	Q 154 RESET			-14.40	
AU1256	Q 154	-9.68			
AU1257	J 221		-8.51	-11.60	-9.75
AU1259	S 154	-6.31			
AU2040	K 359			-9.90	
AU1264	V 154	-6.51			
AU1265	MARSH		-5.49	-9.40	-7.06
AU2042	H 359			-11.20	
AU2043	G 359			-8.90	
AU1268	X 154	-6.25			
AU2044	F 359			-8.50	
AU1274	Z 154	-8.88			
AU1275	A 155	-6.01			
AU1277	B 155 RESET			-13.50	
AU1276	B 155	-5.84			
AU2047	U 358			-7.80	
AU1279		-5.63			
AU2048	C 359			-7.90	
AU1280	THUNDER RM 2		-5.85		
AU1281	THUNDER		-5.51		
AU1283	D 155	-5.52	-5.52		
Mean		**-7.34**	**-7.73**	**-11.27**	**-9.62**

[1] Data provided by Kurt Shinkle (personal commun., 2004).

[2] Data from Shinkle and Dokka (2004).

trends are difficult to detect from the short records spanning only a few years. Despite these limitations, some results of processed data have been presented that indicate that the most recent subsidence rates are substantially lower than those reported for the preceding epoch. Dokka and others (2006) reported that 2002/03 to 2007 average subsidence rates at BVHS, HOUM, and LMCN were -3.5, -4.4, and -6.3 mm/yr, respectively (fig. 26). Prior estimates of subsidence rates at the same locations for the benchmark-releveling epoch of 1966 to 1993 were -15.0, -18.2 and -8.4 mm/yr, respectively (Shinkle and Dokka, 2004). The CORS GPS vertical velocities confirm that subsidence rates in southeastern Louisiana have declined recently, at least at the sites of comparable measurements. The greatest decline in subsidence rates occurred where the prior rates were highest. The average subsidence rates at Boothville, Houma, and Cocodrie now are comparable to or only slightly greater than those that are averaged over geological time scales (Morton and others, 2006; Meckel and others, 2006).

Conclusions and Implications

The core elevations and stratigraphic data indicate that land-water changes at the Barataria basin study areas are products of both marsh-sediment erosion and land subsidence. Erosion exceeded subsidence at most of the former marsh sites that are now open water, except at Fourchon, where the subsidence-erosion predominance was variable depending on core location. At the Bayou Perot study area, erosion exceeded subsidence, but subsidence was greater on the western side of the bayou than on the eastern side. Lower marsh elevations on the west side of Bayou Perot are consistent with subsidence induced by hydrocarbon production from the Delta Farms field complex.

Because comparable methods were used to investigate five study areas in the Barataria basin (this study) and five study areas in the Terrebonne basin (Morton and others, 2005), the results from both basins can be compared. At every study area, peat or organic-rich sediments were recovered in all open-water cores from sites where emergent marshes formerly existed. In general, the results indicate that subsidence primarily caused land-water changes before 1978 in the Terrebonne basin, whereas erosion primarily caused land-water changes after 1978 in the Barataria basin. Even though erosion was greater than subsidence at the Barataria basin sites, the erosion likely was enhanced by initial subsidence that lowered the marsh surface to a position where it was susceptible to erosion by storm waves.

Conversion of marsh to open water at study areas in the Barataria basin occurred after peak hydrocarbon production (figs. 18-22). Land-water changes are consistent with the period of sustained high subsidence rates recorded by the Grand Isle tide gage (fig. 23). A hysteresis of about 10 yr exists between trends of subsidence and wetland loss and trends of hydrocarbon production (Morton and others, 2006; Barras and others, 2008). Data indicate that land-subsidence and wetland-loss rates are closely correlated temporally, but the delay between fluid extraction and peak land-subsidence rates is related to the time it takes for changes in the subsurface to be so great that they manifest as surface changes. In the subsurface, substantial volumes of fluid must be removed and formation pressures substantially reduced before threshold stresses are exceeded and subsidence is induced because of irreversible inelastic compaction of the reservoirs and confining shales. Similarly, once begun, the induced subsidence will continue even after the fluid withdrawal is reduced until the overburden load and pore-fluid pressures re-equilibrate. Consequently, once subsidence was induced, it continued after the rates of hydrocarbon production declined.

The temporal correlations among recent decreases in subsidence rates, wetland loss, and hydrocarbon production support the conclusions of Morton and others (2006) that the accelerated subsidence between 1964 and 1991 was largely induced by long-term, large-volume fluid withdrawal. If only natural processes caused high historical subsidence rates, as reported by Dokka and others (2006) and Gagliano and others (2003), then they should have persisted. This is because salt migration and fault reactivation, which Dokka and others (2006) and Gagliano and others (2003) claimed were responsible for the high subsidence rates, are deep-basin tectonic processes that operate at geological time scales. Although natural internal-basin processes cannot be ruled out entirely, there is no compelling evidence that these processes were responsible for the observed changes. In fact, repeat leveling surveys over the Valentine and Leeville salt domes show historical subsidence (fig. 26B, table 5) rather than the uplift that would be expected if mobilized salt masses were still migrating through the sediment column. On the other hand, if accelerated subsidence was induced by reservoir compaction and fault reactivation associated with fluid withdrawal, which also accelerated in the 1960s and 1970s, then the most recent reductions in subsidence rates would likely reflect a balancing of subsurface stresses and a return to near-equilibrium conditions.

Having extant subsidence rates and understanding their causes are critical for coastal-restoration activities and for modeling and predicting expected impacts of relative sea-level rise on the Mississippi delta. If the historical subsidence trends are natural, then the future trends and rates are uncertain because the temporal variability is unpredictable. Dokka and others (2006) implied that future rates of subsidence would be high if tectonic processes controlled subsidence. In contrast, Morton and others (2006) predicted that subsidence rates would eventually decline to their natural background levels if the high historical subsidence rates were induced. The most recent elevation-change data indicate that high historical subsidence rates in the southern Mississippi delta were anthropogenically induced and should be relatively slow in the future, unless there is a resurgence of subsurface-fluid withdrawal.

Acknowledgments

We thank Jim Flocks, Nick Ferina, and Chandra Dreher (USGS) and Phil McCarty, Mike Brown, and Jeff Motti (University of New Orleans Coastal Research Laboratory) for assisting with fieldwork. John Barras and Blaire Hutchinson rectified several of the aerial photographs used in this report. Michael Bush (River Rest LLC), Mrs. D.E. Jones, Cathy Norman (Wisner Foundation), and Davie Breaux (Greater Lafourche Port Commission) graciously allowed us to collect cores on private lands. Scientific and editorial reviews were provided by Wayne Baldwin and Christopher Reich.

References

Anonymous, 1983, Leeville, Lafourche Parish, *in* Waugespack, S.J. ed., Salt domes of south Louisiana, v. 3: New Orleans Geological Society, p. 44-45.

Barras, J.A., Bernier, J.E., and Morton, R.A., 2008, Land area change in coastal Louisiana – A multidecadal perspective (from 1956 to 2006): U.S. Geological Survey Scientific Investigations Map 3019, scale 1:250,000, 14 p. pamphlet.

Bausfield, John, 1983a, Delta Farms: Lafourche and Jefferson Parishes, Louisiana: New Orleans Geological Society, Oil and Gas Fields of Southeast Louisiana, v. 3, p. 18-18F.

Bausfield, John, 1983b, West Delta Farms: Lafourche and Jefferson Parishes, Louisiana: New Orleans Geological Society, Oil and Gas Fields of Southeast Louisiana, v. 3, p. 19-19B.

Boshart, Bill, 1993, Monitoring Plan for Naomi Outfall Management (BA-03c) and Barataria Bay Waterway East Side Shoreline Protection (BA-26): Louisiana Department of Natural Resources, Coastal Restoration Division, 16 p.

Britsch, L.D., and Dunbar, J.B., 1996, Land loss in coastal Louisiana, Terrebonne Bay, LA: U.S. Army Corps of Engineers Technical Report GL-90-2, Map 6 of 7.

Bronk Ramsey, C., 2001, Development of the radiocarbon calibration program OxCal: Radiocarbon, v. 43, p. 355-363.

Chmura, G.L., Aharon, P., Socki, R.A., and Abernathy, R., 1987, An inventory of ^{13}C abundance in coastal wetlands of Louisiana, USA: Vegetation and sediments: Oecologia, v. 74, p. 264-271.

Day, J.W. Jr., Shaffer, G.P., Britsch, L.D., Reed, D.J., Hawes, S.R., and Cahoon, D.R., 2000, Pattern and process of land loss in the Mississippi Delta: A spatial and temporal analysis of wetland habitat change: Estuaries, v. 23, p. 425-438.

Dokka, R.K., Sella, G.F., and Dixon, T.H., 2006, Tectonic control of subsidence and southward displacement of southeast Louisiana with respect to stable North America: Geophysical Research Letters, 33, L23308, doi: 10.1029/2006GL027250 (online only).

Douglas, B.C., 2001, Sea level change in the era of the recording tide gauge, ch. 3, *in* Douglas, B.C., Kearney, M.S., and Leatherman, S.P., eds., Sea Level Rise – History and Consequences, Academic Press, 228 p.

Federal Geographic Data Committee [prepared for the Federal Geographic Data Committee by the U.S. Geological Survey], 2006, FGDC Digital Cartographic Standard for Geologic Map Symbolization: Reston, Va., Federal Geographic Data Committee Document Number FGDC-STD-013-2006, 290 p., 2 plates.

Gagliano, S.M., Kemp, E.B. III, Wicker, K.M., Wiltenmuth, K.S., and Sabate, R.W., 2003, Neotectonic framework of southeast Louisiana and applications to coastal restoration: Transactions of the 53rd Annual Conference of the Gulf Coast Association of Geological Societies and the Gulf Coast Section SEPM 2003, Baton rouge, LA, October 22-24, 2003, v. 53, p. 262–272.

Greene, A.L., 1998, Successful utilization of 3D seismic at Lafitte Field, southeast Louisiana: Transactions, Gulf Coast Association of Geological Societies, v. 48, p. 159-171.

IHS Inc., 2007, PI/Dwights PLUS on CD, version 1.7: available from IHS Inc., 15 Inverness Way East, Englewood, CO 80112 (*http://energy.ihs.com/Products/Usdata/index.htm*).

Hamilton, W.M., 1983, Barataria Field, Jefferson Parish, Louisiana, *in* McCormick, L.L., and Kline, R.S., eds., Oil and Gas Fields of Southeast Louisiana, v. 3: New Orleans, LA, New Orleans Geological Society, p. 1-1E.

Holdahl, S.R., and Morrison, N.L., 1974, Regional investigations of vertical crustal movements in the U.S. using precise relevelings and mareograph data: Tectonophysics, v. 23, p. 373-390.

Hymel, Melissa, 2003, Monitoring Plan for Barataria Basin Landbridge Shoreline Protection (Phases 1, 2, and 3): Louisiana Department of Natural Resources, Coastal Restoration Division, 10 p.

Jowsey, P.C., 1966, An improved peat sampler: New Phytologist, v. 65, p. 245–248.

Kosters, E.C., Chmura, G.L., and Bailey, A., 1987, Sedimentary and botanical factors influencing peat accumulation in the Mississippi Delta: Journal of the Geological Society, v. 144, p. 423-434.

Kuecher, G.J., 1994, Geologic framework and consolidation settlement potential of the Lafourche Delta, topstratum valley fill: Implications for wetland loss in Terrebonne and Lafourche Parishes, Louisiana: Baton Rouge, LA, Louisiana State University, unpublished Ph.D. dissertation, 375 p.

Kulp, M.A., and Howell, P.D., 1998, Assessing the accuracy of Holocene subsidence rates in southern Louisiana as indicated by radiocarbon-dated peats: Geological Society of America Abstracts with Programs, v. 30 p. 142.

Lanesky, D.E., Logan, B.W., Brown, R.G., and Hine, A.C., 1979, A new approach to portable vibracoring underwater and on land: Journal of Sedimentary Petrology, v. 49, p. 654-657.

Meckel, T.A., ten Brink, U.S., and Williams, S.J., 2006, Current subsidence rates due to compaction of Holocene sediments in southern Louisiana: Geophysical Research Letters, v. 33, L11403, doi:10.1029/2006GL026300 (online only).

Morgan, A.L., 1953, Structural analysis of Delta Farms field, Lafourche Parish, Louisiana: American Association of Petroleum Geologists Bulletin, v. 37, no. 12, p. 2649-2676.

Morton, R.A., Bernier, J.C., and Barras, J.A., 2006, Evidence of regional subsidence and associated interior wetland loss induced by hydrocarbon production, Gulf coast region, USA: Environmental Geology, v. 50, p. 261-274.

Morton, R.A., Bernier, J.C., Barras, J.A., and Ferina, N.F., 2005, Rapid subsidence and historical wetland loss in the Mississippi delta plain: Likely causes and future implications: U.S. Geological Survey Open-file Report 2005-1216, 116 p. (*http://pubs.usgs.gov/of/2005/1216/*).

Morton, R.A., Tiling, G., and Ferina, N.F., 2003, Causes of hotspot wetland loss in the Mississippi delta plain: Environmental Geosciences, v. 10. p. 71-80.

Morton, R.A., and White, W.A., 1997, Characteristics of and corrections for core shortening in unconsolidated sediments: Journal of Coastal Research, v. 13, p. 761-769.

National Research Council, 2006, Drawing Louisiana's new map: The National Academies Press, Washington, D.C., 190 p.

O'Neil, T., 1949, The Muskrat in the Louisiana Coastal Marsh: New Orleans, LA, Louisiana Department of Wildlife and Fisheries, 152 p.

Penland, Shea, Wayne, Lynda, Britsch, L.D., Williams, S.J., Beall, A.D., and Butterworth, V.C., 2000, Process classification of coastal land loss between 1932 and 1990 in the Mississippi River delta plain, southeastern Louisiana: U.S. Geological Survey Open-File Report 00-418, 1 sheet.

Penland, Shea, Ramsey, K.E., McBride, R.A., Mestayer, J.T., and Westphal, K.A., 1988, Relative sea-level rise and delta-plain development in the Terrebonne Parish region: Louisiana Geological Survey, Coastal Geology Technical Report No. 4, 121 p.

Reed, D.J., ed, 1995, Status and trends of hydrologic modification, reduction in sediment availability, and habitat loss/modification in the Barataria-Terrebonne estuarine system: Thibodaux, LA, Barataria-Terrebonne National Estuary Program Publication No. 20, 388 p.

Ritchie, W., and Penland, S., 1985, Overwash process-response characteristics of landforms along the Caminada-Moreau coast, Louisiana, *in* Penland, S. and Boyd, R. eds.,Transgressive depositional environments of the Mississippi River delta plain: A guide to the barrier island, beaches and shoals in Louisiana: Louisiana Geological Survey Guidebook Series No. 3, p. 141-174.

Roberts, H.H., Bailey, A., and Kuecher, G.J., 1994, Subsidence in the Mississippi River delta – Important influences of valley filling by cyclic deposition, primary consolidation phenomena, and early diagenesis: Transactions, Gulf Coast Association of Geological Societies, v. 44, p. 619-629.

Sabate, R.W., 1968, Pleistocene oil and gas in coastal Louisiana: Transactions, Gulf Coast Association of Geological Societies, v. 18, p. 373-386.

Sasser, C.E., Gosselink, J.G., Swenson, E.M., Swarzenski, C.M, and Leibowitz, N.C., 1996, Vegetation, substrate and hydrology in floating marshes in the Mississippi River delta plain wetlands, USA: Vegetatio, v. 122, p. 129-142.

Shinkle, K.D., and Dokka, R.K., 2004, Rates of vertical displacement at benchmarks in the lower Mississippi Valley and the northern Gulf Coast: National Oceanic and Atmospheric Administration Technical Report 50, 135 p.

Swarzenski, C.M., Swenson, E.M., Sasser, C.M., and Gosselink, J.M., 1991, Marsh mat flotation in the Louisiana delta plain: Journal of Ecology, v. 79, p. 999-1011.

Swords, R.M., 1965, Little Lake Field, Jefferson Parish, Louisiana: New Orleans Geological Society, Oil and Gas Fields of Southeast Louisiana, v. 1, p. 116-119.

Wallace, W.E., Jr., 1944, Structure of south Louisiana deep-seated domes: American Association of Petroleum Geologists Bulletin, v. 28, p. 1249-1312.

.

USGS

Morton and others—**Recent Subsidence and Erosion at Diverse Wetland Sites in the Southeastern Mississippi Delta Plain**—Open-File Report 2009-1158

Printed on recycled paper